

# Overview of different characterisations of dynamic heterogeneity

L. Berthier

*Laboratoire des Colloïdes, Verres et Nanomatériaux, Université Montpellier 2 and CNRS UMR 5587, 34095 Montpellier, France*

G. Biroli

*Institut de Physique Théorique, CEA, IPhT, 91191 Gif sur Yvette, France and CNRS URA 2306*

J.-P. Bouchaud

*Science & Finance, Capital Fund Management 6-8 Bd Haussmann, 75009 Paris, France*

R. L. Jack

*Department of Physics, University of Bath, Bath BA2 7AY, United Kingdom*

**OXFORD**  
UNIVERSITY PRESS



# Abstract

Dynamic heterogeneity is now recognised as a central aspect of structural relaxation in disordered materials with slow dynamics, and was the focus of intense research in the last decade. Here we describe how initial, indirect observations of dynamic heterogeneity have recently evolved into well-defined, quantitative, statistical characterisations, in particular through the use of high-order correlation and response functions. We highlight both recent progress and open questions about the characterisation of dynamic heterogeneity in glassy materials. We also discuss the limits of available tools and describe a few candidates for future research in order to gain deeper understanding of the origin and nature of glassiness in disordered systems.

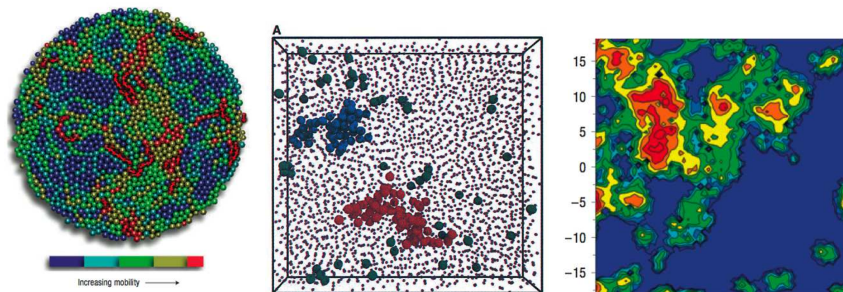


**Fig. 0.1** Three examples of dynamical heterogeneity. In all cases, the figures highlight the clustering of particles with similar mobility. (Left) Granular fluid of ball bearings, with a colour scale showing a range of mobility increasing from blue to red (Keys *et al.*, 2007). (Centre) Colloidal hard sphere suspension, with most mobile particles highlighted (Weeks *et al.*, 2000). (Right) Computer simulation of a two-dimensional system of repulsive disks. The colour scheme indicates the presence of particles for which motion is reproducibly immobile or mobile, respectively from blue to red (Widmer-Cooper *et al.*, 2008).

## 0.1 Introduction

### 0.1.1 Dynamical heterogeneity in glassy materials

The glass transition is often cited as a profound outstanding problem in condensed matter physics. This field may be contrasted with that of simple liquids, for which the broad picture is now well-established, and appropriate theoretical methods are well-developed (Hansen and McDonald, 1986). Why, then, is the glass problem so difficult?

From a theoretical perspective, a central difficulty arises from the importance of fluctuations in glassy systems. Both the liquid and the glass have disordered structure, so even if all molecules in the system are identical, they experience different local environments. In the liquid, these differences can be neglected: one may infer the behaviour of the system from that of a typical particle in a typical environment. Thus, for example, microscopic properties, such as the rate with which particles diffuse in the liquid, are directly related to bulk properties, such as the viscosity. However, as the glass transition is approached, it becomes increasingly difficult to characterise ‘typical’ particles and ‘typical’ environments because a variety of different behaviors emerges. Within a given interval of time, some particles may move distances comparable to their size, while others remain localised near their original positions. Thus, on these time scales, we can refer to ‘mobile’ and ‘immobile’ particles. Of course, on long enough time scales, ergodicity ensures that particles become statistically identical.

In case this discussion seems rather abstract, we refer the reader to Fig. 0.1. Here, we show several systems in which mobile and immobile particles can be identified in particular trajectories using different methods. Strikingly, these images reveal that particles with different mobilities do not appear randomly in space but are clustered. This observation suggests that structural relaxation in disordered systems is a nontrivial dynamical process. In its narrow sense, the term ‘dynamical heterogeneity’ encapsulates the spatial correlations observed in Fig. 0.1. However, the term is frequently

## 2 Preface

used in a broader sense, referring to a range of fluctuation phenomena that arise from deviations from the ‘typical’ behaviour (Ediger, 2000).

Over the last decade, it has become clear from experiments and computer simulations that a variety of glassy systems display the kind of clusters shown in Fig. 0.1. Experimentally, their existence can be inferred from experiments in molecular liquids (Ediger, 2000, Sillescu, 1999, Richert, 2002, Richert *et al.*, 2010), while direct observation of single particle motion makes them vivid in colloids and granular media (Weeks *et al.*, 2000, Keys *et al.*, 2007, Kegel and van Blaaderen, 2000, Dauchot *et al.*, 2005). In computer simulations, spherical particles with simple pair potentials have been used as models for both colloidal and molecular systems, with dynamically heterogeneous behaviour clearly present in a variety of models. Dynamical heterogeneity has also been investigated in a large number of more schematic lattice models, such as kinetically constrained or lattice glass models (Ritort and Sollich, 2003). This important body of experimental and computational observations has also stimulated important theoretical developments since they represent a new set of observations against which existing theories can be confronted.

So far, the reader may be unconvinced of the difficulty of the problem. After all, theoretical methods for analysing systems with large fluctuations and correlated domains already exist: the methods developed to describe critical phenomena, such as field theory and the renormalisation group. These ideas are indeed central to this chapter, but their application to glassy liquids has required substantial new insight into the nature of the relevant fluctuations and observables. The reason is that the distinction between mobile and immobile particles is in essence dynamical. Therefore, if one analyses static snapshots of viscous liquids, there is little evidence of increasing fluctuations or heterogeneity, at least when analysed using standard liquid state correlation functions. Instead of an ensemble of snapshots, one must apply the methods of critical phenomena to an ensemble of ‘movies’ (i.e. trajectories, or dynamical histories) of the system. This will be the approach that we will follow in later sections.

### 0.1.2 Suitable probes for the emergence of glassiness

Returning to Fig. 0.1, the observation of clusters of mobile particles (or at least of regions with correlated mobility) raises many questions. What is the nature of the clusters? Indeed, are they of the same nature in each case? What determines their size? How is their size distribution related to the relaxation time of the system, if at all? Do the particles in fast or slow clusters have different local environments that can be characterised by any simple structural measure? From a theoretical point of view, it is natural to ask whether the correlated regions represent the cooperatively rearranging regions imagined long ago by Adam-Gibbs (Adam and Gibbs, 1965); whether they mirror some soft elastic modes in the system; how they might connect to locally-ordered domains; or whether they reveal the presence of localised defects that facilitate structural rearrangement.

However, before addressing these ambitious questions, we must answer a more prosaic one. How can the ‘clusters of mobile and immobile particles’ be defined and characterised? In Fig. 0.1, the mobile particles were identified by a threshold on their displacement, over a particular time scale. Indeed, many early papers have suggested

different ways to define ‘mobility’ and ‘clusters’ that are similar in spirit but different in practice, as we detail in the following sections. However, one must certainly evaluate how strongly the cluster properties depend on thresholds or time scales, which might hinder firm conclusions and may prevent fair comparison between different systems.

In more recent years, it has become possible to define and measure observables that can be determined without arbitrariness in a range of systems, are amenable to analytic theory and scaling arguments, and may sometimes be inferred from experimental data even in molecular liquids. These are known as ‘four-point correlation functions’ and are now broadly accepted as standard tools for analysing dynamical heterogeneity.

Within this toolbox, a central role is played by the four-point dynamical susceptibility  $\chi_4(t)$ . Loosely speaking, it measures the number of particles involved in correlated motion on times scales of the order of  $t$ . To interpret the dynamical susceptibility, it is useful to invoke an analogy with critical phenomena, in which a (static) correlation length  $\xi$  diverges at a critical temperature  $T_c$ , accompanied by the spontaneous appearance of an order parameter. This divergence is associated with a diverging susceptibility  $\chi$ , which may be measured either through the fluctuations of the order parameter or through the response of the order parameter to its conjugate field. When considering such phenomena in glasses, a problem arises, in that a static order parameter and its conjugate field are not known. Instead, a fairly good dynamical order parameter is given by any generic dynamical two-point correlator, e.g. density-density, displaying the slowing down of the dynamics. This motivated the use of a four-point dynamical susceptibility associated to spontaneous fluctuations of the dynamical order parameter. This allows the identification of a dynamic length scale,  $\xi_4(t)$ , and a susceptibility,  $\chi_4(t)$ , by analogy with conventional critical phenomena.

Returning to Fig. 0.1, simulation studies and recent experiments indicate that the clustering of mobile particles is directly linked with an increasing susceptibility  $\chi_4$  and an increasing correlation length scale  $\xi_4$ . The central part of this chapter will be devoted to a discussion of these four-point functions. We will discuss some of the insights that they have revealed into the nature of glassy behaviour in liquids, colloids, and granular media. However, these studies also revealed that interpretation of four-point functions may be somewhat ambiguous, while direct measurements of correlation length scales remain difficult. Additionally, the averaging procedure inherent in the four-point functions means that they may obscure important features of dynamic heterogeneity such as the cluster shape and the nature of interfaces between clusters of mobile and immobile particles. Towards the end of the chapter, we will discuss a range of alternative observables that complement the information available from four-point functions.

## 0.2 Observables for characterising dynamical heterogeneity

### 0.2.1 Two-point observables and their inadequacy

We begin with a review of some two-point functions that are used to characterise simple liquids. We will show that these functions are largely blind to the dynamically heterogeneous behaviour shown in Fig. 0.1, motivating the discussion of more

#### 4 Preface

discriminating observables<sup>1</sup>.

For any fluid of particles, a natural quantity to measure is the structure factor,

$$S(q) = \frac{1}{N} \langle \rho_{\mathbf{q}}(t) \rho_{-\mathbf{q}}(t) \rangle, \quad (0.1)$$

where brackets indicate an ensemble average, and the Fourier component of the density is

$$\rho_{\mathbf{q}}(t) = \sum_{i=1}^N e^{i\mathbf{q} \cdot \mathbf{r}_i(t)}, \quad (0.2)$$

with  $N$  being the number of particles and  $\mathbf{r}_i(t)$  being the position of particle  $i$  at time  $t$ . The structure factor gives information about the strength of density fluctuations on a length scale  $2\pi/|\mathbf{q}|$ . However, its behaviour in the vicinity of the glass transition is unremarkable, with no hint of the dynamic clustering of Fig. 0.1. Although static heterogeneities in the density would directly imply the existence of dynamic heterogeneity, the reverse is not true. Thus, dynamic heterogeneity related to the motion of particles has a much more subtle origin. Note that more complicated static correlation functions have been studied (Debenedetti, 1996), especially in numerical work, all attempting to identify fluctuations of some prescribed sort of local order (translational, orientational, etc.). Until now, there are no strong indications of a diverging, or even substantially growing, lengthscale (Menon and Nagel, 1995, Fernandez *et al.*, 2006). In order to see the growth of a static amorphous correlation, one possibility is to introduce the so-called ‘‘point-to-set’’ correlation function that we discuss later, see section 0.4.4.

We therefore turn to dynamical observables. A quantity relevant for light and neutron scattering experiments is the intermediate scattering function,

$$F(\mathbf{q}, t) = \frac{1}{N} \langle \rho_{\mathbf{q}}(t) \rho_{-\mathbf{q}}(0) \rangle. \quad (0.3)$$

Measurements of this function by neutron scattering in supercooled glycerol (Wuttke *et al.*, 1996) are shown for different temperatures in Fig. 0.2. These curves suggest a first, rather fast, relaxation to a plateau followed by a second, much slower, relaxation. The plateau is due to the fraction of density fluctuations that are frozen on intermediate timescales, but eventually relax during the second relaxation. The latter is called ‘alpha-relaxation’, and corresponds to the structural relaxation of the liquid. The plateau is akin to the Edwards-Anderson order parameter, defined for spin glasses which measures the fraction of frozen spin fluctuations (Binder and Kob, 2005). Note that the Edwards-Anderson parameter continuously increases from zero below the critical temperature in the conventional spin glass transition (Mézard *et al.*, 1988), while for structural glasses, a finite plateau value seems to emerge above any putative transition.

The full decay of the intermediate scattering function can be measured only within a relatively small range of temperatures. In order to track the dynamic slowing down

<sup>1</sup>There are other examples of systems for which standard two-point correlators are blind to interesting intermittent (or heterogeneous) effects, such as turbulence or financial markets, and for which higher order correlations are informative.

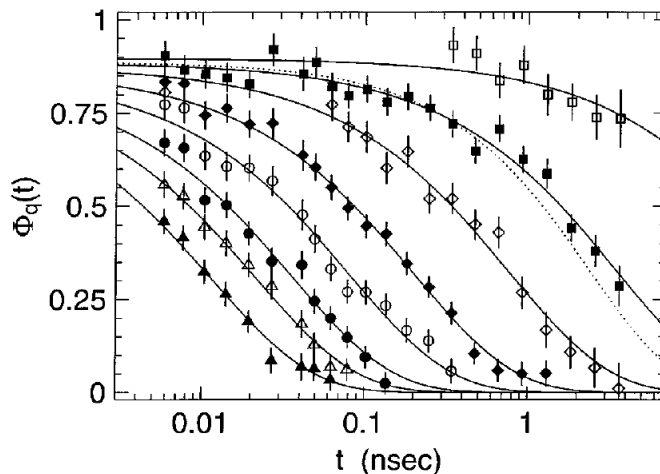


**Fig. 0.2** Temperature evolution of the normalised intermediate scattering function,  $\phi_{\mathbf{q}}(t) = S(\mathbf{q}, t)/S(\mathbf{q}, 0)$ , for supercooled glycerol (Wuttke *et al.*, 1996). Temperatures decrease from 413 K to 270 K from left to right. The lines are fits with a stretched exponential form.

from microscopic to macroscopic timescales, other correlators have been studied. A very popular one is the measurement of the dielectric linear susceptibility which can be followed over up to 18 decades of frequency (Lunkenheimer and Loidl, 2002). It is generally accepted that different dynamic probes reveal similar temperature dependences for the relaxation time, at least as long as the probes measure local motion. In broad terms, the essential features on supercooling are a dramatic increase in the correlation time, and a broad distribution of time scales in the system characterised in the time-domain by non-exponential relaxation functions.

It is increasingly accepted that the presence of such broad distributions of time scales in glassy systems is associated with the presence of mobile and immobile domains. However, the size and shape of these domains, or even their very existence, cannot be deduced directly from  $F(\mathbf{q}, t)$ . We are therefore motivated to consider more advanced correlation functions.

### 0.2.2 Indirect evidence: Intermittency and decoupling phenomena

We now return to the presence of mobile and immobile particles in the supercooled phase. Simulation studies are ideal for studying fluctuation properties, since accurate trajectories for all particles are accessible, over long time scales. These features are displayed in Fig. 0.3, which shows that while the averaged mean-squared displacements are smooth functions of time, time signals for individual particles clearly exhibit specific features that are not observed unless dynamics is resolved both in space and time. In this figure, we observe that particle trajectories are very intermittent, being composed of a succession of long periods of time where particles simply vibrate around well-defined locations, separated by rapid ‘jumps’. Vibrations were previously inferred

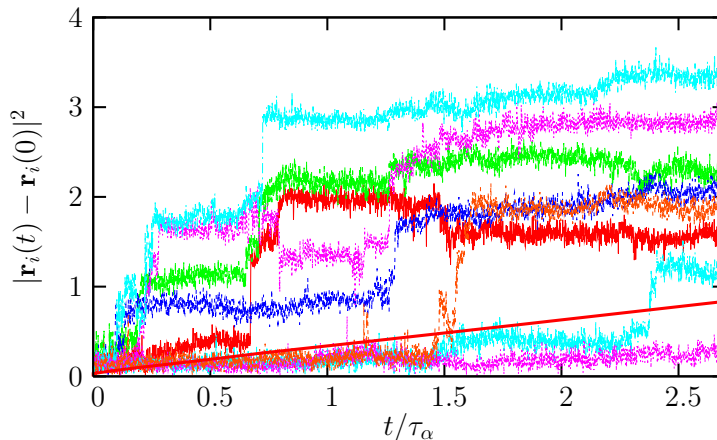


**Fig. 0.3** Time resolved squared displacements of individual particles in a simple model of a glass-forming liquid composed of Lennard-Jones particles (Berthier and Kob, 2007). The average is shown as a smooth full line and time is expressed in units of structural relaxation time  $\tau_\alpha$ . Trajectories are composed of long periods of time during which particles vibrate around well-defined positions, separated by rapid jumps that are statistically widely distributed in time, underlying the importance of dynamic fluctuations.

from the plateaux observed at intermediate times in the mean squared displacements or intermediate scattering functions, but the existence of jumps that are statistically widely distributed in time cannot be revealed from averaged quantities only. The fluctuations in Fig. 0.3 suggest, and direct measurements confirm, the importance played by fluctuations around the averaged dynamical behaviour to understand structural relaxation in glassy materials.

Remaining at the single particle level, these fluctuations can be characterised through the (time-dependent) distribution of particle displacements. This is the self-part of the van-Hove function, defined as

$$G_s(\mathbf{r}, t) = \left\langle \frac{1}{N} \sum_{i=1}^N \delta(\mathbf{r} - [\mathbf{r}_i(t) - \mathbf{r}_i(0)]) \right\rangle. \quad (0.4)$$

For an isotropic Gaussian diffusive process, one has  $G_s(\mathbf{r}, t) \sim \exp\left(-\frac{|\mathbf{r}|^2}{4D_s t}\right)$ . While simple liquids are well-described by such a distribution, simulations of glassy systems instead reveal strong deviations from Gaussian behaviour on the timescales relevant for structural relaxation (Kob *et al.*, 1997). In particular they reveal ‘broad’ tails in the distributions that are much wider than expected from the Gaussian approximation. These tails are in fact well described by an exponential, rather than Gaussian, decay in a wide time window comprising the structural relaxation,

$$G_s(\mathbf{r}, t) \sim \exp\left(-\frac{|\mathbf{r}|}{\lambda(t)}\right), \quad (0.5)$$

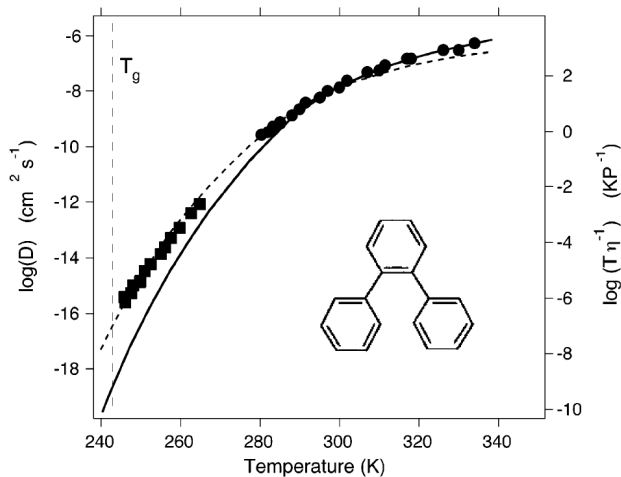


**Fig. 0.4** Decoupling between viscosity (full line) and self-diffusion coefficient (symbols) in supercooled ortho-terphenyl (Mapes *et al.*, 2006). The dashed line shows a fit with a ‘fractional’ Stokes-Einstein relation,  $D_s \sim (T/\eta)^\zeta$  with  $\zeta \sim 0.82$  instead of the expected value  $\zeta = 1$ .

which is a direct consequence of the intermittent motion shown in Fig. 0.3 (Chaudhuri *et al.*, 2007). These tails reflect the existence of a population of particles that moves distinctively further than the rest and appears therefore to be much more mobile. This observation implies that relaxation in a viscous liquid differs qualitatively from that of a normal liquid where diffusion is close to Gaussian, and that a non-trivial statistics of single particle displacements exists in materials with glassy dynamics.

Another influential phenomenon that was related early on to the existence of dynamic heterogeneity is the decoupling of self-diffusion ( $D_s$ ) and viscosity ( $\eta$ ). In the high temperature liquid, self-diffusion and viscosity are related by the Stokes-Einstein relation (Hansen and McDonald, 1986),  $D_s\eta/T = \text{const}$ . For a large particle moving in a fluid the constant is equal to  $1/(6\pi R)$  where  $R$  is the particle radius. Physically, the Stokes-Einstein relation means that two different measures of the relaxation time,  $R^2/D_s$  and  $\eta R^3/T$ , lead to the same timescale up to a constant factor. In supercooled liquids this phenomenological law breaks down, as shown in Fig. 0.4 for ortho-terphenyl (Mapes *et al.*, 2006). It is commonly found that  $D_s^{-1}$  does not increase as fast as  $\eta$  so that, at  $T_g$ , the product  $D_s\eta$  has significantly increased as compared to its Stokes-Einstein value. The Stokes-Einstein ‘violation’ factor is larger for more fragile liquids, and can be as high as  $10^3$ . This phenomenon, although less spectacular than the overall change of viscosity, is a strong indication that different ways to measure relaxation times lead to different answers and, thus, is a strong hint of the existence of broad distributions of relaxation timescales (Stillinger and Hodgdon, 1994, Tarjus and Kivelson, 1995).

Indeed, a natural explanation of this effect is that different observables probe the

underlying distribution of relaxation times in different ways (Ediger, 2000). For example, the self-diffusion coefficient of tracer particles is dominated by the more mobile particles whereas the viscosity or other measures of structural relaxation probe the timescale needed for every particle to move. An unrealistic but instructive example is a model where there is a small, non-percolative subset of particles that are blocked forever, coexisting with a majority of mobile particles. In this case, the structure never fully relaxes but the self-diffusion coefficient is non-zero because of the mobile particles. Although unrealistic since all particles move in a viscous liquid, this example shows how different observables are likely to probe different moments of the distribution of timescales, as explicitly shown within several theoretical frameworks (Tarjus and Kivelson, 1995, Jung *et al.*, 2004, Hedges *et al.*, 2007, Heuer, 2008).

### 0.2.3 Early studies of dynamic heterogeneity

The phenomena described above, although certainly an indication of spatio-temporal fluctuations, do not allow one to study how these fluctuations are correlated in space. However, this is a fundamental issue both from the experimental and theoretical points of view, as discussed in the introduction. To discriminate between different explanations of glassy behaviour, it would be useful to know: How large are the regions that are faster or slower than the average? How does their size depend on temperature? Are these regions compact or fractal?

These important questions were first addressed in pioneering works using four-dimensional NMR (Tracht *et al.*, 1998, Reinsberg *et al.*, 2001), and by directly probing fluctuations at the nanoscopic scale using microscopy techniques. In particular, Vidal Russel and Israeloff used Atomic Force Microscopy techniques (Vidal Russell and Israeloff, 2000) to measure the polarisation fluctuations in a volume of size of few tens of nanometers in a supercooled polymeric liquid (PVAc) close to  $T_g$ . In this spatially resolved measurement, the hope is to probe a small enough number of dynamically correlated regions, and to detect their dynamics. Indeed, the time signals shown in Ref. (Vidal Russell and Israeloff, 2000) show a very intermittent dynamics, switching between moments with intense activity, and moments with no dynamics at all, suggesting that extended regions of space indeed transiently behave as fast and slow regions. A much smoother signal would have been measured if dynamically correlated ‘domains’ were not present.

Spatially resolved and NMR experiments are quite difficult. They give undisputed information about the typical lifetime of the dynamic heterogeneity, but their determination of a dynamic correlation lengthscale is rather indirect, and has been performed on a small number of liquids in narrow temperature windows. Nevertheless, an agreed consensus is that these experiments reveal the existence of a non-trivial dynamic correlation length emerging at the glass transition, where it reaches a value of the order of 5 to 10 molecule diameters (Ediger, 2000).

More recently, studies of systems for which single-particle dynamical data is available have led to direct observation of clusters of mobile particles, such as those shown in Fig. 0.1. This is possible in materials where the particles are big enough to be visualised through microscopy, such as colloids, or with a camera, such as granular materials. In early studies, mobile and immobile particles were usually identified by using a threshold on their displacement within a given time interval, dividing the par-

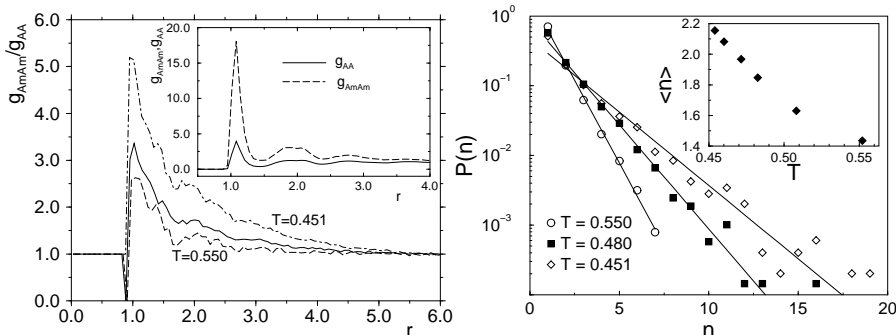


**Fig. 0.5** Early measurements of dynamical heterogeneity from computer simulation. (Left) The main figure shows the probability that a particle is within the active population, given that it is a distance  $r$  from another active particle (Kob *et al.*, 1997). The increasing correlation between active particles is apparent on decreasing the temperature. (Right) The length distribution of string-like clusters of active particles (Donati *et al.*, 1998).

ticles into sub-populations. This then allows characterisation of correlations within the populations, as shown in Fig. 0.5. For example, ratios of radial distribution functions give the probability that particles in the vicinity of a mobile particle are themselves mobile. Other work concentrated for instance on the morphology and size of clusters of mobile particles, as shown in Fig. 0.5.

Results such as those of Fig. 0.5 gave clear evidence of large fluctuations and dynamical heterogeneity. However, unambiguous identification of a mobile population of particles proved difficult, with most distributions of mobility showing broad but unimodal distributions. Similarly, the identification of connected clusters of mobile particles introduces further ambiguity into the data processing, with their size and shape depending quite strongly on the definition of the mobile population. To achieve unambiguous and system-independent definitions of length scales and correlation volumes, it is useful to define correlation functions that do not involve separating particles into distinct populations, nor the identification of connected clusters. Four-point functions are a natural choice in this regard, and will be discussed in the next chapter.

#### 0.2.4 Higher order correlations: four-point functions

*Definitions.* In the previous section, we considered the probability that a particle is within some mobile population, given that it has a mobile particle a distance  $r$  away (recall Fig. 0.5). While the measurement of such a probability requires the identification of a mobile population, there is a straightforward alternative which contains similar information. We first define a continuously varying ‘mobility’  $c_i(t, 0)$  which indicates how far or how much particle  $i$  moves between times  $t = 0$  and  $t$ . Then, given two particles at separation  $r$ , one can measure the degree to which their mobilities are correlated. To this end, it is convenient to define a ‘mobility field’ through (Bennemann *et al.*, 1999, Donati *et al.*, 1999, Glotzer *et al.*, 2000)

$$c(\mathbf{r}; t, 0) = \sum_i c_i(t, 0) \delta(\mathbf{r} - \mathbf{r}_i). \quad (0.6)$$

## 10 Preface

Then, the spatial correlations of the mobility are naturally captured through the correlation function (Dasgupta *et al.*, 1991)

$$G_4(r; t) = \langle c(\mathbf{r}; t, 0)c(\mathbf{0}; t, 0) \rangle - \langle c(\mathbf{r}; t, 0) \rangle^2, \quad (0.7)$$

which depends only on the single time  $t$  and the single distance  $r = |\mathbf{r}|$  as long as the average is taken at equilibrium in a translationally invariant system. The analogy with fluctuations in critical systems becomes clear in Eq. (0.7) if one considers the mobility field  $c(\mathbf{r}; t, 0)$  as playing the role of the order parameter for the transition, characterised by non-trivial fluctuations and correlations near the glass transition.

Often, the mobility  $c_i(t, 0)$  is itself a two-point function. For example, to measure mobility on a length scale  $2\pi/q$ , one might consider  $o_i(q, t) = e^{i\mathbf{q}\cdot\mathbf{r}_i(t)}$  and  $c_i(t, 0) = o_i(\mathbf{q}, t)o_i(-\mathbf{q}, 0)$ . In this case,  $o_i(\mathbf{q}, t)$  is related to a Fourier component of the density of the system, and the average of  $c_i(t, 0)$  is the self-part of the intermediate scattering function  $F(\mathbf{q}, t)$  defined in Eq. (0.3). Moving from a particle observable  $o_i(\mathbf{q}, t)$  to a field  $o(\mathbf{r}; \mathbf{q}, t)$ , one arrives at

$$G_4(r; t) = \langle o(\mathbf{r}; \mathbf{q}, t)o(\mathbf{r}; -\mathbf{q}, 0)o(\mathbf{0}; \mathbf{q}, t)o(\mathbf{0}; -\mathbf{q}, 0) \rangle - \langle o(\mathbf{r}; \mathbf{q}, t)o(\mathbf{r}; -\mathbf{q}, 0) \rangle^2. \quad (0.8)$$

This correlation function is quartic in the operator  $o$ , so it is known as a ‘four-point function’. It measures correlations on a length scale  $r$ , associated with motion between time zero and time  $t$ ; it depends additionally on the length scale  $q^{-1}$  used in the definition of the particle mobility  $c_i(t, 0)$ . Since structural relaxation typically involves particle motion over a distance comparable to the particle size  $R$ , one typically chooses  $q \sim 1/R$  and studies the remaining  $t$  and  $r$  dependences.

This definition of a real-space correlation function of the mobility represents a vital advance in the characterisation of dynamical heterogeneity. In particular, it allows the language of field theory and critical phenomena to be used in studying dynamical fluctuations in glassy systems. By analogy with critical phenomena, if there is a single dominant length scale  $\xi_4$  then one expects that for large- $r$ , the correlation function decays as

$$G_4(r; t) \sim \frac{A(t)}{r^p} e^{-r/\xi_4(t)}, \quad (0.9)$$

with  $p$  an exponent whose value is discussed below. It is also natural to define the susceptibility associated with the correlation function

$$\chi_4(t) = \int dr G_4(r; t). \quad (0.10)$$

If the prefactor  $A(t)$  were known, the susceptibility  $\chi_4(t)$  could be used to extract the typical number of particles involved in correlated motion. That is,  $\chi_4(t)$  may be interpreted as the size of the correlated clusters in Fig. 0.1.

Further,  $\chi_4(t)$  can also be obtained from the fluctuations of the total mobility  $C(t, 0) = \int d^d\mathbf{r} c(\mathbf{r}; t, 0)$ , through

$$\chi_4(t) = N[\langle C(t, 0)^2 \rangle - \langle C(t, 0) \rangle^2]. \quad (0.11)$$

In practice, this formula allows an efficient measure of the degree of dynamical heterogeneity, at least in computer simulations and in experiments where the dynamics

can be spatially and temporally resolved. As long as the observable  $c(\mathbf{r}; t, 0)$  is chosen appropriately, this observable can be measured in a wide variety of systems, and serves as a basis for fair comparisons of the extent of dynamical heterogeneity.

*The spin glass perspective: four-point functions in space and time.* It is interesting to note that four-point functions have their origin in spin glass physics, where they were used to investigate the onset of long-ranged amorphous order. The key insight is due to Edwards and Anderson (Edwards and Anderson, 1975). In a spin glass, one considers a set of  $N$  localised degrees of freedom, the spins, which we denote by  $s_x$ , with  $x$  denoting the position in space. The spins interact by quenched random couplings. Then, two-point correlation functions between spins such as  $\sum_x \langle s_x s_{x+r} \rangle$  typically vanish for  $r \neq 0$ , since sites separated by a distance  $r$  may be either correlated or anti-correlated, with equal probability. The Edwards-Anderson solution is to consider instead the static spin-glass correlation  $\chi_{SG} = N^{-1} \sum_x \langle s_x s_{x+r} \rangle^2$  which receives a positive contribution for both correlated and anti-correlated sites.

If one then considers a four-point dynamic function such as

$$G_4(r; t) = \frac{1}{N} \sum_x \langle s_x(0) s_{x+r}(0) s_x(t) s_{x+r}(t) \rangle, \quad (0.12)$$

then this approaches the static spin-glass correlation at long times. In spin glasses, spontaneous symmetry breaking occurs into an amorphous solid with long-ranged order at a second order spin glass transition. Near such a phase transition,  $G_4(r; t)$  obeys critical scaling behaviour similar to that shown by static correlation functions near familiar phase transitions, and the corresponding susceptibility  $\chi_4(t)$  diverges.

In structural glasses, the possibility of a static transition to an amorphous ordered state remains highly controversial. However, four-point functions such as  $G_4(r; t)$  and  $\chi_4(t)$  can be usefully employed in the fluid state to characterise dynamical fluctuations, regardless of their possible connection to any critical point.

*Four-point susceptibilities in molecular, colloidal and granular glasses.* The function  $\chi_4(t)$  has been measured in computer simulations of many different glass-forming liquids, by molecular dynamics, Brownian and Monte Carlo simulations, see e.g. (Bennemann *et al.*, 1999, Donati *et al.*, 1999, Glotzer *et al.*, 2000, Franz *et al.*, 1999, Lacevic *et al.*, 2003, Berthier, 2004, Vogel and Glotzer, 2004, Berthier, 2007, Parisi, 1999, Parsaeian and Castillo, 2008). An example is shown in Fig. 0.6 for a Lennard-Jones liquid. The qualitative behaviour is similar in all cases (Franz and Parisi, 2000, Toninelli *et al.*, 2005, Berthier *et al.*, 2007a): as a function of time  $\chi_4(t)$  first increases, it has a peak on a timescale that tracks the structural relaxation timescale and then it decreases. As mentioned above, the decrease of  $\chi_4(t)$  at long times constitutes a major difference with spin glasses. In a spin glass,  $\chi_4$  would be a monotonically increasing function of time whose long-time limit coincides with the static spin glass susceptibility. Physically, the difference is that the spin glass state which emerges at the transition is critical or marginally stable, i.e. characterized by singular static responses.

The peak value of  $\chi_4(t)$  measures the volume over which the structural relaxation processes are correlated. Therefore, the most important result obtained from data such as presented in Fig. 0.6 is the temperature evolution of the peak height, which is found

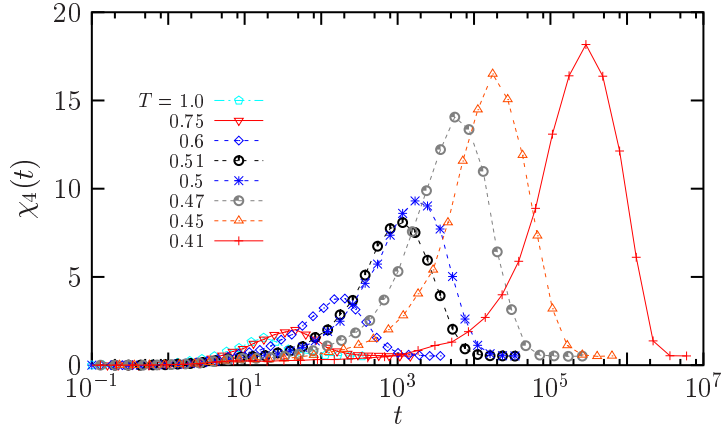


**Fig. 0.6** Time dependence of  $\chi_4(t)$  quantifying the spontaneous fluctuations of the self-intermediate scattering function in a molecular dynamics simulation of a Lennard-Jones supercooled liquid (Berthier, 2004). For each temperature,  $\chi_4(t)$  has a maximum, which shifts to larger times and has a larger value when  $T$  is decreased, revealing the increasing lengthscale of dynamic heterogeneity in supercooled liquids approaching the glass transition.

to increase when the temperature decreases and the dynamics slows down. From such data, one gets direct evidence that the approach to the glass transition is accompanied by the development of increasingly long-ranged spatial correlations of the dynamics. Note that if the dynamically correlated regions were compact, the peak of  $\chi_4$  would be proportional to  $\xi_4^d$  (in  $d$  spatial dimensions), thus directly relating  $\chi_4(t)$  measurements to that of the relevant lengthscale  $\xi_4$  of dynamic heterogeneity.

In experiments, direct measurements of  $\chi_4(t)$  have been made in colloidal (Weeks *et al.*, 2007) and granular materials (Dauchot *et al.*, 2005, Keys *et al.*, 2007) close to the colloidal and granular glass transitions, and also in foams (Mayer *et al.*, 2004) and gels (Duri and Cipelletti, 2006), because dynamics is more easily spatially and temporally resolved in those cases. The results obtained in all these cases are again broadly similar to those shown in Fig. 0.6, both for the time dependence of  $\chi_4(t)$  and its evolution upon a change of the relevant variable controlling the dynamics.

A major issue is that obtaining information on the behaviour of  $\chi_4(t)$  and  $G_4(r; t)$  from experiments on molecular systems is difficult. In molecular liquids, it remains a difficult task to resolve temporally the dynamics at the nanometer scale. Such measurements are however important because numerical simulations and experiments on colloidal and granular systems can typically only be performed for relaxation times spanning at most 5-6 decades. On the other hand, in molecular liquids, up to 14 decades can be measured, and extrapolation of simulation data all the way to the experimental glass transition is fraught with difficulty. Indirect estimates of  $\chi_4(t)$  from experiments will be discussed below.

These results are also relevant because many theories of the glass transition assume or predict, in one way or another, that the dynamics slows down because there are increasingly large regions over which particles have to relax in a correlated or cooper-

ative way, see Sec. 0.3.2 and Ref. (Tarjus, 2010). However, this lengthscale remained elusive for a long time. Measures of the spatial extent of dynamic heterogeneity, in particular  $\chi_4(t)$  and  $G_4(r; t)$ , seem to provide the long-sought evidence of this phenomenon. This in turn suggests that the glass transition can indeed be considered as a form of critical phenomenon involving growing time scales and length scales. This is an important progress towards the understanding of the glass transition phenomenon, even though a clear and conclusive understanding of the relationship between dynamic lengthscales and relaxation timescales is still the focus of intense research.

*Dependence of  $\chi_4(t)$  on the observable and probe length scale.* As discussed above, one may define a four-point function  $G_4(r; t)$  starting from any suitable mobility  $c(\mathbf{r}; t, 0)$ . Indeed, many candidates have been considered. It is not our intention to give a detailed list, but a few comments are in order.

A natural choice for  $\chi_4(t)$  is to start from Eq. (0.11) and to take  $C(t, 0) = \rho_{\mathbf{q}}(t)\rho_{-\mathbf{q}}(0)$  as the autocorrelation of a single Fourier component of the density. In this case, the average of  $C(t, 0)$  is the intermediate scattering function  $F(\mathbf{q}, t)$  of Eq. (0.3). In computational studies, it is often more convenient to construct instead  $C(t, 0)$  from a simple sum over particles. That is, one defines the single-particle mobility

$$f_i(\mathbf{q}, t, 0) \equiv e^{i\mathbf{q}\cdot(\mathbf{r}_i(t) - \mathbf{r}_i(0))}, \quad (0.13)$$

whose average is the self-part of  $F(\mathbf{q}, t)$ . The real-space four-point function is then given by Eq. (0.7), and the definition of  $\chi_4(t)$  follows. These two definitions of  $\chi_4(t)$  are not equivalent. Differences between them were discussed in Ref. (Lacevic *et al.*, 2003), where it was concluded that they contain similar information.

Physically speaking, the key point is that as particle  $i$  moves away from its initial position  $r_i(0)$ , the function  $f_i(\mathbf{q}; t, 0)$  decays from a value of unity, reaching zero when the particle has moved a distance of order  $(\pi/|\mathbf{q}|)$ . Once the particle has moved further than this, the oscillations in the cosine function imply that averages of  $f_i$  give numbers close to zero. Based on this physical interpretation, other choices for  $c_i(t, 0)$ , including step functions, or smoothly decaying functions were used (Franz *et al.*, 1999, Bennemann *et al.*, 1999, Lacevic *et al.*, 2003, Berthier, 2004). As expected on physical grounds, constructing four-point functions based on these choices for  $c_i(t, 0)$  again leads to qualitatively similar behaviours.

Yet another choice is to use a function  $c_i(t, 0)$  that depends not just on the positions at time zero and time  $t$ , but also on the whole history of the particle between these times. In particular, one may take a ‘persistence’ function which takes a value of unity if the particle remains within a distance  $a$  of its initial position for all times between 0 and  $t$ ; otherwise it takes the value zero. Again, one observes a broadly similar behaviour (Chandler *et al.*, 2006).

All these choices for the definition of the local mobility  $c_i(t, 0)$  involve a ‘probe length scale’, which is fixed by the choice of measurement, in contrast to the sought dynamic length scale  $\xi_4(t)$  which should be a physical property of the system. While the specific form of  $c(\mathbf{r}; t, 0)$  is typically unimportant for the qualitative behaviour of four-point functions, the quantitative results do depend on the probe length scale.

Typically, if the probe length scale  $a$  is of the order of the particle diameter or smaller,  $c(\mathbf{r}; t, 0)$  measures local motion, and this is often the scale on which heterogene-

ity is most apparent. As the probe length scale is increased, contributions to  $\chi_4(t)$  come from pairs of particles that remain correlated over distances comparable to  $a$  and, typically, such correlations weaken as  $a$  increases, reducing  $\chi_4(t)$  (Chandler *et al.*, 2006). Similarly, reducing  $a$  also reduces  $\chi_4(t)$  as short-scale motion corresponding to thermal vibrations are also typically uncorrelated. Therefore,  $\chi_4(t)$  is usually maximal for a probe length scale comparable to the particle size, and it is fixed to a constant when comparing data at different temperatures or densities. An alternative choice is to adjust the probe lengthscale  $a$  at different state points such that  $\chi_4(t; a)$  reaches its absolute maximum, this can be very important for some systems like granular media close to the rigidity transition where the maximum is reached for values of the probe length far below the particle size (Lechenault *et al.*, 2008a, Lechenault *et al.*, 2008b, Heussinger *et al.*, 2010).

*Real-space measurements and associated structure factors.* We concluded above that a growing peak in  $\chi_4(t)$  ‘directly’ reveals the growth of a dynamic correlation lengthscale as the glass transition is approached. This can only be correct if the assumptions made above for the scaling form of  $G_4(r; t)$  are correct. Dynamic lengthscales should in principle be obtained by direct measurements of a spatial correlation function (Doliwa and Heuer, 2000, Lacevic *et al.*, 2002).

However, in contrast to  $\chi_4(t)$ , detailed measurements of  $G_4(r; t)$  are technically more challenging as dynamic correlations must now be resolved in space over large distances with a very high precision, and so there is much less data to draw on. From the point of view of numerical simulations where many measurements of  $\chi_4$  were reported, the main limitation to properly measure  $\xi_4$  is the system size. This might seem surprising as typical numbers extracted for the correlation length scale  $\xi_4$  are modest, growing, say, from 1 to at most 5-10 in most reports. However, this modest number hides the fact that the correlation function only decays to zero for distances  $r$  that are several times larger than  $\xi_4$ . Given that  $G_4(r; t)$  is accurately measured up to  $r = L/2$  in a periodic system of linear size  $L$ , going to few  $\xi_4$  (say, five times), when  $\xi_4 \sim 5$  requires systems containing at least  $N \sim L^3 \sim (2 \times 5 \times 5)^3 \sim 10^5$  particles in three dimensions, assuming the density is near  $\rho \approx 1$ . Such large system sizes are not easily studied at low temperatures when relaxation times get very large, even with present day computers. However, these studies are of vital importance in that they allow the dynamical length scale  $\xi_4(t)$  to be measured directly. Moreover, insights from such studies can then be used when inferring the behaviour of  $\xi_4(t)$  from measurements of  $\chi_4(t)$ .

Some representative data are shown in Fig. 0.7. They are obtained for a lattice gas model with kinetic constraints, where measurements of  $G_4(r; t)$  are somewhat easier than in molecular dynamics simulations. As discussed above, the idea is that for large  $r$ ,  $G_4(r; t) \simeq A(t)r^{-p}F(r/\xi_4(t))$  which then yields

$$\chi_4(t) \simeq A(t)\xi_4(t)^{d-p}. \quad (0.14)$$

Often, one estimates the prefactor  $A(t)$  to be equal to  $G_4(0, t)$ , which is simply the variance of the local quantity  $c(r; 0, t)$ . However, the accuracy of this estimate is hard to assess without explicit evaluation of  $G_4(r, t)$ . In the example shown in Fig. 0.7,

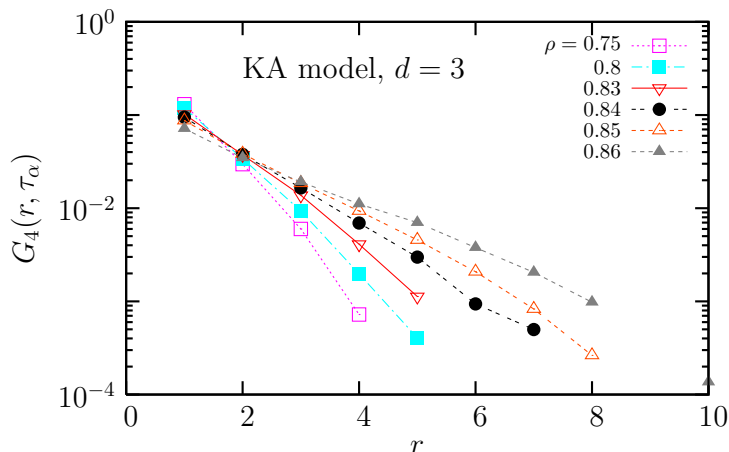


**Fig. 0.7** Four-point correlation function  $G_4(r; t = \tau_\alpha)$  measured in computer simulations of the Kob-Andersen kinetically constrained lattice gas in three dimensions (Berthier, 2003). The dynamics slows down when density  $\rho$  increases, and the slower spatial decay of  $G_4$  directly reveals increasingly longer ranged dynamic correlations accompanying the glass transition.

for instance the scaling between  $\chi_4$  and  $\xi_4$  in Eq. (0.14) is well obeyed, and careful examination of  $G_4(r; t)$  suggests that  $p \approx 1$  and  $A$  is indeed a constant of order 1.

While this is a subtle situation which requires each case to be considered individually, the work in this domain is broadly consistent with  $\chi_4(t)/G_4(0, t)$  representing the number of particles involved in heterogeneous relaxation. Note that these issues will also be relevant for discussion of other correlations and susceptibilities in later sections. Therefore, truly ‘direct’ measurements indeed confirm that the increase of the peak of  $\chi_4(t)$  corresponds, as expected, to a growing dynamic lengthscale  $\xi_4(t)$  (Doliwa and Heuer, 2000, Lacevic *et al.*, 2002, Bennemann *et al.*, 1999, Berthier, 2004, Berthier *et al.*, 2007a). As a result of subtleties related to the difference between four-point correlations in spin glasses and structural glasses, an early study of four-point functions (Dasgupta *et al.*, 1991) drew an opposite conclusion, but the data of that study are in fact consistent with the now-established picture of a growing length scale.

We also note, in passing, that the power  $p$  may have more than one interpretation. Typically, one assumes that a typical cluster has size  $\xi_4(t)$  and contains  $\xi_4(t)^{d-p}$  particles, so that  $d-p$  is interpreted as a fractal dimension. However, an alternative would be that clusters are all compact, but that the distribution of their sizes is rather broad. This uncertainty reflects the fact that four-point functions involve averages over many clusters, so that they do not resolve details of cluster structure.

Instead of direct inspection of  $G_4(r; t)$ , it is often convenient to consider its Fourier transform  $S_4(k; t) = \int d^d r e^{i\mathbf{k}\cdot\mathbf{r}} G_4(r; t)$  (Bennemann *et al.*, 1999, Donati *et al.*, 1999, Glotzer *et al.*, 2000, Lacevic *et al.*, 2002, Berthier, 2004, Yamamoto and Onuki, 1998a, Yamamoto and Onuki, 1998b, Flenner and Szamel, 2010). In particular, this allows data for different times and different temperatures to be combined into a scaling analysis that can yield the temperature dependence of  $\xi_4$ , leaving an uncertain prefac-

tor. This approach was taken for example in Refs. (Yamamoto and Onuki, 1998*b*, Berthier *et al.*, 2007*a*, Flenner and Szamel, 2010). Typically, simulation data result in length scales between 1 and 5 diameters.

So far, we have considered circularly-averaged  $G_4(r; t)$  and  $S_4(k; t)$ . However, if the probe function  $c_i(t, 0)$  is anisotropic, as in Eq. (0.13), four-point functions  $G_4(r; t)$  then also depend on the angle between the separation vector  $\mathbf{r}$  and the probe vector  $\mathbf{q}$ . Several papers (Weeks *et al.*, 2007, Flenner and Szamel, 2009, Doliwa and Heuer, 2000) have investigated this issue and found that motion in longitudinal directions is indeed more strongly correlated than motion in transverse directions, such that  $G_4(r; t)$  is truly an anisotropic function. These findings add further to the difficulty of extracting the length scale  $\xi_4$  from direct measurements of four-point structure factors.

### 0.2.5 Experimental estimates of multi-point susceptibilities

Although readily accessible in numerical simulations, the fluctuations of  $C(t, 0)$  that give access to  $\chi_4(t)$  are in general very small and impossible to measure directly in experiments, except when the range of the dynamic correlation is macroscopic, as in granular materials (Marty and Dauchot, 2005) or in soft glassy materials where it can reach the micrometer and even millimetre range (Mayer *et al.*, 2004, Duri and Cipelletti, 2006). To access  $\chi_4(t)$  in molecular liquids, one should perform time-resolved dynamic measurements probing very small volumes, with a linear size of the order of a few nanometers. Although possible, such experiments remain to be performed with the required accuracy.

It was recently realized that simpler alternative procedures exist. The central idea underpinning these results is that induced dynamic fluctuations are in general more easily accessible than spontaneous ones, and both types of fluctuations can be related to one another by fluctuation-dissipation theorems. The physical motivation is that while four-point correlations offer a direct probe of the dynamic heterogeneities, other multi-point correlation functions give very useful information about the microscopic mechanisms leading to these heterogeneities.

For example, one might expect that the slow part of a local enthalpy (or energy, density) fluctuation  $\delta h_x(t = 0)$  at position  $x$  and time  $t = 0$  triggers or eases the dynamics in its surroundings, leading to a systematic correlation between  $\delta h_x(t = 0)$  and  $c(x + r; t, 0)$ . This physical intuition suggests the definition of a family of three-point correlation functions that relate thermodynamic or structural fluctuations to dynamical ones. Interestingly, and crucially, some of these three-point correlations are both experimentally accessible and give bounds or approximations to the four-point dynamic correlations (Berthier *et al.*, 2005, Berthier *et al.*, 2007*a*, Berthier *et al.*, 2007*b*).

Based on this insight, one may obtain a lower bound on  $\chi_4(t)$  using the Cauchy-Schwartz inequality  $\langle \delta H(0) \delta C(t, 0) \rangle^2 \leq \langle \delta H(0)^2 \rangle \langle \delta C(t, 0)^2 \rangle$ , where  $H(t)$  denotes the enthalpy at time  $t$ , and  $\delta X = X - \langle X \rangle$  denotes the fluctuating part of the observable  $X$ . By using a fluctuation-dissipation relation valid when the energy is conserved by the dynamics, the previous inequality can be rewritten as (Berthier *et al.*, 2005):

$$\chi_4(t) \geq \frac{k_B T^2}{c_P} [\chi_T(t)]^2, \quad (0.15)$$

where the multi-point response function  $\chi_T(t)$  is defined by

$$\chi_T(t) = \left. \frac{\partial \langle C(t, 0) \rangle}{\partial T} \right|_{N, P} = \frac{N}{k_B T^2} \langle \delta H(0) \delta C(t, 0) \rangle, \quad (0.16)$$

and  $c_P$  is the specific heat per particle (at constant pressure).

In this way, the experimentally accessible response  $\chi_T(t)$  which quantifies the sensitivity of average correlation functions  $\langle C(t, 0) \rangle$  to an infinitesimal temperature change, can be used in Eq. (0.15) to yield a lower bound on  $\chi_4(t)$ . From Eq. (0.16), it is clear that  $\chi_T$  is directly related to the covariance of enthalpy and dynamic fluctuations, and thus captures the part of dynamic heterogeneity which is triggered by enthalpy fluctuations.

Detailed numerical simulations and theoretical arguments (Berthier *et al.*, 2007*a*, Berthier *et al.*, 2007*b*) strongly suggest that the right hand side of (0.15) actually provides a good estimate of  $\chi_4(t)$  in supercooled liquids, and not just a lower bound. Similar estimates exist considering density as a perturbing field instead of the temperature. These are useful when considering colloidal or granular materials where the glass transition is mostly controlled by the packing fraction. The quality of the corresponding lower bound was tested experimentally on granular packings close to the jamming transition (Lechenault *et al.*, 2008*b*), and numerically for colloidal hard spheres (Brambilla *et al.*, 2009).

Using this method, Dalle-Ferrier *et al.* (Dalle-Ferrier *et al.*, 2007) have been able to estimate the evolution of the peak value of  $\chi_4$  for many different glass-formers in the entire supercooled regime. In Fig. 0.8 we show some of these results as a function of the relaxation timescale. The value on the  $y$ -axis, a bound on the peak of  $\chi_4$ , is a proxy for the number of molecules,  $N_{\text{corr},4}$  in a cluster of mobile or immobile particles. As discussed briefly above,  $\chi_4(t)$  is expected to be equal to  $N_{\text{corr},4}$ , up to a proportionality constant  $A(t)$  which is not known from experiments, probably explaining why the high temperature values of  $N_{\text{corr},4}$  are smaller than one. Figure 0.8 also indicates that  $N_{\text{corr},4}$  grows faster when  $\tau_\alpha$  is not very large, close to the onset of slow dynamics, and a power law relationship between  $N_{\text{corr},4}$  and  $\tau_\alpha$  is good in this regime ( $\tau_\alpha/\tau_0 < 10^4$ ). The growth of  $N_{\text{corr},4}$  with  $\tau_\alpha$  becomes much slower closer to the glass transition temperature  $T_g$ , where a change of 6 decades in time corresponds to a mere increase of a factor about 4 of  $N_{\text{corr},4}$ , suggesting logarithmic rather than power law growth of dynamic correlations. A similar crossover towards a very slow growth of dynamic correlations is reported for colloidal hard spheres (Brambilla *et al.*, 2009) and model glasses (Berthier *et al.*, 2007*a*), and is observed in numerical simulations even if the dynamic lengthscale  $\xi_4$  is directly estimated (Flenner and Szamel, 2010). The consequences of such an effect for theories of the glass transition are discussed below. Bearing in mind all the caveats discussed above (unknown prefactors, quality of the bound, etc.), the experimental data compiled in Fig. 0.8 do appear to confirm that dynamic fluctuations and correlation lengthscales do grow when the molecular liquids approach their glass transitions.

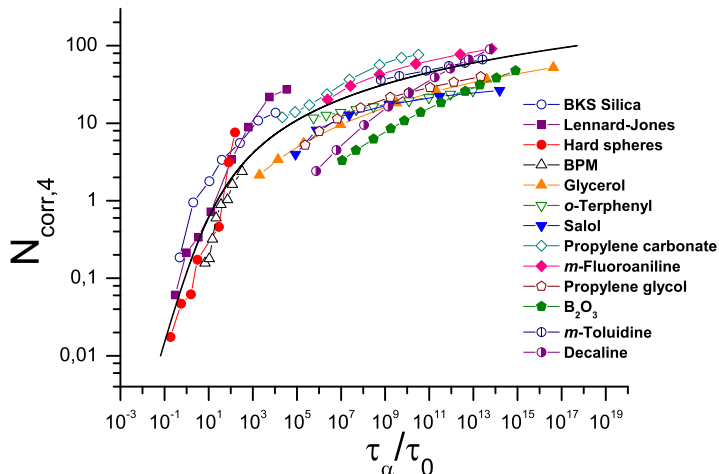


**Fig. 0.8** Dynamic scaling relation between the number of dynamically correlated particles,  $N_{\text{corr},4}$ , and relaxation timescale,  $\tau_\alpha$ , for a number of glass-formers (Dalle-Ferrier *et al.*, 2007), determined using the bound provided by Eq. (0.15). For all systems, dynamic fluctuations increase when the glass transition is approached. The full line through the data (Dalle-Ferrier *et al.*, 2007) suggests a crossover from algebraic,  $N_{\text{corr},4} \sim \tau_\alpha^z$ , to logarithmic,  $N_{\text{corr},4} \sim \exp(\tau_\alpha^\psi)$ , growth of dynamic correlations with increasing  $\tau_\alpha$ .

### 0.2.6 Four-point susceptibilities: some caveats

The above story about the four-point susceptibility looks quite enticing. We have essentially argued that dynamical heterogeneity should be quantified by the spatial correlations of the mobility. This correlation function is a priori hard to measure in molecular glasses, but a divine surprise occurs: using rather trivial mathematics, its spatial integral is found to be bounded from below by a quantity that is much easier to measure. Is this too good to be true? What is the physics underpinning this ‘easy’ bound?

The answer is that four-point correlation functions pick up a contribution that depends both on the statistical ensemble used (i.e. NVE vs. NVT) and on the dynamics (i.e. Brownian vs. Newtonian). Using general scaling arguments based on a dominant length scale  $\xi_4$ , one can show that in Fourier space the four-point correlation function has the following structure (in the  $k \rightarrow 0$  limit) (Berthier *et al.*, 2007a, Berthier *et al.*, 2007b):

$$S_4(k; \tau_\alpha) = \xi_4^s \hat{H}_1(k\xi_4) + g(k) \left[ \xi_4^s \hat{H}_2(k\xi_4) \right]^2, \quad (0.17)$$

where  $s$  is a certain exponent (related to  $p$  above through  $2s = d - p$ ) and  $\hat{H}_{1,2}$  are certain scaling functions which behave similarly at small and large arguments. The

wavevector dependent function  $g(k)$  carries the dependence on the statistical ensemble and dynamics. In particular,  $g(k=0) = 0$  when all conserved quantities are strictly fixed, as in the NVE ensemble<sup>2</sup>. Similarly,  $g(k)$  is very different for Brownian dynamics (for which energy is not conserved) or for Newtonian dynamics (that conserves energy). So one has to face the uneasy truth that  $\chi_4(t) \equiv S_4(k=0; t)$  depends on many microscopic and macroscopic details, although physically these should not affect the dynamic correlation length  $\xi_4$ . It is definitely not so easy to directly relate  $\chi_4$  to a dynamic correlation length. Intuitively, conserved variables play a role in “transmitting” the information about mobility from one region to another.

From the above expression, one sees that  $S_4(k; t)$  mixes up two contributions that one would like to disentangle so as to extract the relevant scaling contribution from the first term only. It turns out that this first term is proportional to a three-point response function, that measures the change of the dynamics induced by a perturbation some distance away, and that we will discuss in more detail in section 0.4. It is this three-point response, not  $G_4$ , that is the fundamental object carrying information about dynamical heterogeneities, and from which  $G_4$  is constructed. The space integral of the three-point response function is  $\xi_4^s \hat{H}_1(0)$ ; physically it represents the response of the dynamics to a uniform shift of an external parameter, such as the temperature or the density. Hence  $\chi_T(t)$  as defined in the previous section is a three-point function at zero wavevector. This explains the physical nature of the lower bound on  $\chi_4(t)$ : due to the contribution of the energy as a conserved quantity,  $\chi_4$  has two contributions: one proportional to  $\chi_T$  and one proportional to  $\chi_T^2$ , the latter being precisely the lower bound of the previous section.

This discussion leads to the following caveats, that we alluded to above: a) the identification of a correlation volume from  $\chi_4(t)$  alone is not warranted in general. The information contained in  $S_4(k; \tau_\alpha)$  is needed to unambiguously relate the growth of  $\chi_4(t)$  to a growing lengthscale;<sup>3</sup> b) extracting information from  $S_4$  can be difficult due to interference effects between the two terms and c) three-point response functions are the fundamental building bricks for dynamic correlations, and are not soiled with problems related to conserved variables or statistical ensembles.

## 0.3 Theoretical discussion

### 0.3.1 Recent progress based on four-point functions

In the previous section, we have summarised some of the properties of four-point functions, their advantages for calculating the extent of dynamical heterogeneity, and some direct and indirect measurements of these quantities.

There are many subtleties associated with these measurements, but the same broad picture is observed in a variety of systems and is robust to the precise measurement used. Essentially, as relaxation times increase, the four-point susceptibility increases,

<sup>2</sup>Actually, fast degrees of freedom can give subleading contributions in some cases.

<sup>3</sup>Related to this point, it is worth mentioning the case of purely Arrhenius systems, which are considered to be non-cooperative systems. Still, the lower bound based on  $\chi_T$  proves that  $\chi_4(\tau_\alpha)$  diverges in these systems as least as  $T^{-2}$  as the temperature goes to zero (Dalle-Ferrier *et al.*, 2007). The physical interpretation of such an apparent growth of the range of dynamical correlations is still unclear.

suggesting the presence of a growing dynamic correlation length. Where the real-space function  $G_4(r; t)$  can also be measured, this confirms more directly the increase of such a length scale, typically in the range between 1 and 10 molecular diameters. The fundamental, unavoidable conclusion seems to be that glassy behaviour is not a purely local ‘caging’ of particles by their neighbours, but indeed a genuine collective phenomenon.

Having established the existence of a growing correlation length, several questions arise. From a theoretical perspective, we are familiar with the idea, borrowed from equilibrium critical phenomena, that when correlation length scales get large, microscopic features of the system become unimportant, and ‘universal’ behaviour emerges. Whether realistic glassy systems have length scales that are large enough for such a universal description remains unclear. Many analyses in this spirit have nevertheless been attempted, as we shall discuss shortly. It is likely that in order to reach a good quantitative agreement a careful treatment of pre-asymptotic effects will have to be performed.

A second fundamental point concerns the microscopic mechanisms that give rise to the correlations revealed by four-point functions. Many model systems can demonstrate the presence of increasing time scales, coupled with increasing susceptibilities  $\chi_4(t)$  and length scales  $\xi_4$ . Predictions from different theoretical frameworks of the form of four-point functions are discussed in the next section, and we evaluate some of the theories in the light of existing results.

### 0.3.2 Models of the glass transition and their predictions of dynamic heterogeneity

We now turn to perhaps the most fundamental question in this area: what are the dominant mechanisms by which structural relaxation takes place in glassy materials? We give a quick survey of the dominant pictures for molecular glasses, their predictions for four-point functions, and the extent to which these are borne out.

*Mode-coupling theory.* The mode-coupling theory (MCT) of the glass transition (Götze and Sjögren, 1995) was historically derived from liquid state theory. Starting from exact microscopic equations of motion for the density field in a liquid, several uncontrolled approximations are then performed to yield a closed set of dynamical equations for intermediate scattering functions. These equations give rise to a dynamic singularity at some finite temperature,  $T_c$ , where relaxation times diverge in an algebraic manner. Additionally, very precise quantitative predictions can be made about the specific form of intermediate scattering functions, suggesting a very rich behaviour of time correlation functions, which do resemble the behaviour observed experimentally and reported in Fig. 0.2. As is well-known these predictions only apply over a modest time window of about 2-3 decades in the moderately supercooled regime, but dramatically break down nearer to the glass transition (Götze, 2008).

Another dramatic failure of the traditional formulation of the theory, more relevant to the present contribution, is its inability to accurately predict the shape of the van-Hove distribution function described above, the resulting wavevector dependence of the self-intermediate scattering function (especially at low wavevector), and the corresponding decoupling between self-diffusion constant and the viscosity.

Following this historical route, therefore, it is not obvious whether the MCT dynamic singularity is accompanied by non-trivial dynamic fluctuations. This also means that the theory is not easily interpreted in physical terms. Recently, mode-coupling theory was reformulated in such a way that both these issues were greatly clarified. Using a field-theoretic formulation, it is possible to perform consistent mode-coupling approximations to get analytical predictions for both averaged two-time dynamic correlation functions and for the dynamic fluctuations around the averaged behaviour, i.e. for  $\chi_4(t)$  (Franz and Parisi, 2000, Berthier *et al.*, 2007b, Biroli and Bouchaud, 2004). In a subsequent recent move, ‘inhomogeneous mode-coupling’ predictions for the shape and scaling form of four-point spatial correlation functions  $G_4(r; t)$  and its Fourier transform  $S_4(k; t)$  were finally obtained (Biroli *et al.*, 2006). Thus, overall, mode-coupling theory is now able to make an impressive set of very detailed predictions for a very large family of spatio-temporal correlation functions for any given liquid, starting from the form of the microscopic interaction between the particles.

A few numerical simulations have been presented to test these new predictions. First, the temporal evolution of the four-point susceptibility  $\chi_4(t)$  was compared to mode-coupling predictions. Just as time-correlation functions decay within MCT in a two-step process similar to the data presented in Fig. 0.2,  $\chi_4(t)$  is predicted to grow with time with two distinct power laws,  $\chi_4 \sim t^a$  and  $\chi_4 \sim t^b$  in the time regimes respectively corresponding to the approach to, and departure from, the plateau. These two power law regimes have been successfully identified in numerical work, with numerical values for the exponents  $a$  and  $b$  that are in ‘reasonable’ agreement with numbers predicted by MCT (Berthier *et al.*, 2007b, Berthier, 2007, Berthier and Kob, 2007).

The peak of the four-point susceptibility is predicted to diverge algebraically at the critical temperature. This prediction was observed numerically to hold over a similar (restricted) temperature window as for the averaged relaxation time  $\tau_\alpha$  itself. This finding implies that the peak of  $\chi_4$ , when plotted as a function of  $\tau_\alpha$ , follows a power law scaling,  $\chi_4 \sim \tau_\alpha^z$ , where  $z$  is predicted to be a non-universal critical exponent. Returning to the data compilation in Fig. 0.8, we remark that the data obtained in the moderately supercooled regime do indeed approximately follow an initial growth which is consistent with the MCT prediction, while clearly breaking down at lower temperatures.

Finally, predictions for the detailed shape of four-point correlation functions, in particular for  $S_4(k; t)$ , were recently confronted to numerical results, with inconclusive results. While a first paper (Stein and Andersen, 2008) reports excellent agreement with MCT predictions both for the wavevector dependence of  $S_4(k; t)$  and its evolution with temperature, a more recent report (Karmakar *et al.*, 2009) claims that disagreements with theoretical predictions arise when larger system sizes are included in the numerical analysis. This ongoing debate illustrates the fact mentioned above that even for the modest correlation length scales characterising relaxation in supercooled liquids, very large system sizes are needed to unambiguously and accurately measure four-point functions. Clearly, more work is needed to clarify the status of the large body of MCT predictions regarding four-point functions.

*Facilitation picture and kinetically constrained models.* In the facilitation picture of supercooled liquids, structural relaxation is thought to originate from propagation of

localised excitations, or ‘defects’, throughout the system (Glarum, 1960). The idea is that the local structure at position  $x$  changes rapidly when a defect visits the neighbourhood of  $x$ . Then, one makes the further hypothesis that defects are sparse, and most of the system is in fact immobile, such that defects can be considered as uncorrelated, independent objects. In practice, very little is known about the nature, origin, or even the existence of such defects in real liquids.

Nevertheless, it is clear within this picture that dynamics is highly heterogeneous in space, and temporally intermittent. Physically, one expects a dynamic correlation lengthscale  $\xi_4$  to emerge, which should basically correspond to the linear size of the region explored independently by a given defect. This also means that the time dependence of  $\xi_4(t)$ , and thus of  $\chi_4(t)$  can directly be connected, in this view, to how fast the defects move. In the simplest approximation where defects are diffusive objects, one would expect  $\xi_4(t) \sim \sqrt{t}$  for  $t < \tau_\alpha$ .

In recent years, these ideas have been pursued quite extensively, based on the proposal (Garrahan and Chandler, 2003) that facilitation is essential for explaining the heterogeneous dynamics of supercooled liquids. The theory has been developed primarily through studies of systems called kinetically constrained models (Ritort and Sollich, 2003). Numerous distinct lattice models belong to this family, which can be distinguished by the set of microscopic rules governing the dynamics of the localised defects, the existence or absence of conservation laws, the topology of the lattice, etc. The simplest models, such as the (one-spin facilitated) Fredrickson-Andersen (FA) model, in fact reproduce nearly exactly the scaling relations mentioned above for four-point functions (Toninelli *et al.*, 2005, Chandler *et al.*, 2006, Whitlam *et al.*, 2004, Whitlam *et al.*, 2005).

Given the large number of distinct models, and the fact that models are postulated instead of being derived as approximate, coarse-grained representations of liquids, it is not clear how one should compare their behaviour to numerical results obtained for realistic liquid models. This issue is discussed in a recent review (Chandler and Garrahan, 2010). Thus, it is perhaps better to interpret this diversity as being suggestive of the different types of behaviour one can possibly encounter in liquids. On the other hand, from the theoretical point of view, having well-defined, relatively simple, statistical models defined on the lattice is very appealing as very many detailed and quantitative results can be obtained by exploiting tools from statistical mechanics. Thus, kinetically constrained models can also be viewed as ‘toy supercooled liquids’.

In this regard, the study of the dynamically heterogeneous behaviour of kinetically constrained models has been a very active field of research in recent years. Many models have been investigated and a large number of time correlation functions (two-point, four-point, persistence functions) have been analysed, suggesting possible behaviours for dynamic susceptibilities (Berthier *et al.*, 2007a, Chandler *et al.*, 2006) or decoupling phenomena (Jung *et al.*, 2004, Pan *et al.*, 2005). We refer to the chapter by Sollich, Toninelli, and Garrahan for further details and references on this topic.

At the qualitative level, it is obvious that all models are characterised by rapidly growing time scales and length scales, and are thus interesting models to study dynamic heterogeneity. However, models with diffusive point defects (like the simplest of Fredrickson-Andersen models), do not compare well with the real liquids that have been studied so far. In three dimensions, they predict simple exponential relaxation

and no decoupling phenomena (Jack *et al.*, 2006). The dependence of  $\chi_4$  on time and temperature are also characterised by scaling laws that have not been observed in numerical and experimental results (Toninelli *et al.*, 2005, Berthier *et al.*, 2005). However, the Arrhenius scaling of their relaxation time indicates a relation between these models and ‘strong’ liquids (Garrahan and Chandler, 2003, Whitlam *et al.*, 2005) and there are comparatively few results on dynamical heterogeneity for such materials. In particular, while such models predict rather large dynamical length scales in strong materials (Garrahan and Chandler, 2003, Berthier and Garrahan, 2005), these have not yet been observed.

On the other hand, more complicated models where defects move sub-diffusively or cooperatively seem to be more appropriate representations of ‘fragile’ liquids, which have a non-Arrhenius scaling of relaxation time with temperature. Such kinetically constrained models exhibit stretched exponential relaxation as in Fig. 0.2, decoupling phenomena (Jung *et al.*, 2004) similar to the results in Fig. 0.4, realistic form of four-point structure factors as in Fig. 0.7, or dynamic length scales which grow very slowly (Garrahan and Chandler, 2003), in qualitative agreement with the experimental results shown in Fig. 0.8.

*Adam-Gibbs and the mosaic picture.* The idea that relaxation events in glasses are collective and involve the simultaneous motion of several particles dates back at least to Adam and Gibbs, who provided an argument to relate the size of these “cooperatively rearranging regions” (CRR) to the configurational entropy of the supercooled liquid. A lot of the work on dynamical heterogeneities is in fact motivated by the Adam-Gibbs picture and attempts to determine the size of these CRR (Binder and Kob, 2005).

The Adam-Gibbs picture was later put on more solid ground in the context of the Random First Order Transition (RFOT) Theory of glasses (Kirkpatrick *et al.*, 1989, Lubchenko and Wolynes, 2006). RFOT suggests that supercooled liquids can be thought of as a mosaic of “glass nodules” or “glassites” with a spatial extension  $\ell^*(T)$  limited by the configurational entropy. Regions of size smaller than  $\ell^*(T)$  are ideal glasses: they cannot relax, even on very long time scales, because the number of states towards which the system can escape is too small to compete with the energy that blocks the system in a given favourable configuration. Regions of size greater than  $\ell^*$  are liquid in the sense that they explore with time an exponentially large number of unrelated configurations, and all correlation functions go to zero. The relaxation time of the whole liquid is therefore the relaxation time of glassites of size  $\ell^*$ . This relaxation occurs through collective activated events that sweep a region of size  $\ell^*$ , which are the CRR regions of the Adam-Gibbs theory. The crucial assumption of RFOT is that thermodynamics alone fixes the value of  $\ell^*$ , whereas the relaxation time  $\tau_\alpha$  involves the height of the activation barriers on scale  $\ell^*$ , which is assumed to grow as a power-law,  $\ell^{*\psi}$ , where  $\psi$  is a certain exponent (Bouchaud and Biroli, 2004).

Note that when an activated event takes place within a glassite of size  $\ell^*$ , the boundary conditions of the nearby region changes. There is a substantial probability that this triggers, or facilitates, an activated event there as well, possibly inducing an “avalanche” process that extends over the dynamic correlation length scale  $\xi > \ell^*$ . The dynamics on length scales less than  $\ell^*$  is, within RFOT, inherently cooperative, but the relation between the dynamic correlation length  $\xi$ , defined for example through

three- or four-point correlation function and the mosaic length  $\ell^*$  is at this stage an important open problem (see (Dalle-Ferrier *et al.*, 2007, Capaccioli *et al.*, 2008)). If  $\xi$  is of the order of a few glassite lengths  $\ell^*$ , then one expects that  $\chi_4(\tau_\alpha)$  should grow as  $\ell^*$  to some power. Assuming activated scaling,  $\ln \tau_\alpha \sim \ell^{*\psi}$ , finally leads to  $\chi_4 \sim (\ln \tau_\alpha)^z$ , instead of a power-law relation predicted by MCT or by non-cooperative KCMs. The crossover towards this logarithmic behaviour is not incompatible with the data (Xia and Wolynes, 2000), see section 0.2.5 above. In fact, the details of the crossover between the MCT region and the RFOT region are still very mysterious (see (Biroli and Bouchaud, 2009) for a recent discussion), but some claims have been made about the evolution of the shape of the dynamically correlated regions, that should morph from stringy, fractal objects in the MCT region to compact blobs at lower temperatures (Stevenson *et al.*, 2006). It would be interesting to devise some experimental protocol to test these predictions.

## 0.4 Beyond four-point functions: other tools to detect dynamical correlations

So far, we have discussed how four-point functions can be used to estimate dynamical length scales, and we have stated that these are typically found to be in the range 1-10 molecular diameters. However, we have also noted that (a) the four-point susceptibility estimate of the dynamical correlation volume may lead to erroneous results (see section 0.2.6) and (b) a variety of different theories of the glass transition are broadly consistent with the above estimate.

To make further progress, it seems that more adapted and discriminating observables will be required. In fact, there are a wealth of methods that have been used to characterise dynamical heterogeneity, of which we discuss just a few, and we refer to other chapters in this book for details. Here, we mainly emphasise the questions that can be addressed by different methods, and give an overview of the relationships between some of the methods that have been developed in different contexts.

### 0.4.1 Non-linear susceptibilities

In standard critical phenomena, diverging two-point correlations lead to singular linear responses. It is therefore quite natural to conjecture that increasing dynamical correlations should also lead to anomalous responses of some kind. Spin glass theory provides, again, an interesting insight. As discussed in section 0.2.4 the spin glass transition (at zero external field) is signaled by the divergence of the four-point static correlation function  $\chi_{SG}$ . It can be easily established that close to the transition,  $\chi_{SG}$  is related to the third-order non-linear magnetic response at zero frequency  $\chi_3(\omega = 0)$  (Fischer and Hertz, 1991):

$$\chi_3(\omega = 0) = -\frac{\chi_{SG} - 2/3}{(k_B T)^2}. \quad (0.18)$$

Thus, although linear responses are blind to the development of spin glass long range order, the non-linear magnetic response is not. Actually, it diverges at the transition and, hence, is a direct experimental probe, contrary to  $\chi_{SG}$ , which can instead only be measured in numerical simulations.

The analogy with spin glasses discussed in section 0.2.4 therefore suggests that glasses should also display increasingly non-linear responses approaching the glass transition, as first argued in (Bouchaud and Biroli, 2005). Theoretically, this can be substantiated by some general scaling arguments and by a mode-coupling calculation. These are described in (Tarzia *et al.*, 2010); we will just briefly summarize them in the following. The starting point is to rewrite the generic third order non-linear response  $\chi_3(t)$  in terms of the second order change  $R_2$  of the linear response  $R$ :

$$\begin{aligned} \chi_3(t) &= \int_{-\infty}^t dt_1 dt_2 dt_3 \frac{\delta P(t)}{\delta E(t_1) \delta E(t_3) \delta E(t_2)} E(t_1) E(t_2) E(t_3) = \\ & \int_{-\infty}^t dt_1 dt_2 dt_3 E(t_1) \frac{\delta R(t, t_1)}{\delta E(t_2) \delta E(t_2)} E(t_2) E(t_3) = \int_{-\infty}^t dt_1 E(t_1) R_2(t, t_1) \end{aligned} \quad (0.19)$$

Note that we will focus on the dielectric non-linear response (so  $P$  is the electric polarization) but the generalization to other perturbing field is straightforward<sup>4</sup>. It is easy to understand, at least at low frequency, why  $R_2$  and therefore the non-linear susceptibility have a singular behavior. In fact, within an adiabatic approximation, one finds that the linear response in the steady state created by a slowly alternating field is:

$$R_{eq}(t - t', E \cos(\omega t)), \quad (0.20)$$

where  $R_{eq}(t - t', E)$  is the equilibrium response function with a *static* field  $E$ . Since we are interested in the small  $E$  behavior, we can expand the above expression up to second order in  $E$ , this yields:

$$R_2(t, t_1) = R_{eq}(\tau, E \cos(\omega t)) - R_0(\tau) \approx \frac{E^2 \cos^2(\omega t)}{2} \left. \frac{\partial^2 R_{eq}(t - t_1, E)}{\partial E^2} \right|_{E=0}, \quad (0.21)$$

where  $R_0(\tau)$  is the unperturbed equilibrium response function, and the derivative is computed with respect to a constant external field. The second term is expected to give a singular contribution because close to the glass transition a small applied field  $E$  is roughly equivalent to a shift of the order of  $E^2$  of the glass transition temperature (see below), and  $\tau_\alpha$  significantly varies when the temperature is changed by a small amount close to  $T_g$ . More precisely, by taking into account the  $E \rightarrow -E$  symmetry one can rewrite  $\partial^2 R_{eq} / \partial E^2$  as  $2 \partial R_{eq} / \partial \Theta$  where  $\theta = E^2$ . Using the time temperature superposition, one finds:

$$\left. \frac{\partial R_{eq}(\tau, E)}{\partial \Theta} \right|_{E=0} \simeq \kappa \frac{\partial R_{eq}(\tau, 0)}{\partial T}. \quad (0.22)$$

where  $\kappa = \frac{\partial \tau_\alpha / \partial \Theta}{\partial \tau_\alpha / \partial T}$ . Using that  $R_{eq}(\tau, 0)$  is the Fourier transform of the linear susceptibility  $\chi_1(\omega)$  and plugging the previous expressions in (0.19) (and after some algebra detailed in (Tarzia *et al.*, 2010)) one finds the following result:

<sup>4</sup>Depending on the perturbing field, the symmetry  $E \rightarrow -E$  will hold or not. In the latter case, the first non-linear response is the quadratic one, in the former the quadratic vanishes by symmetry and one has to focus on the third order one.

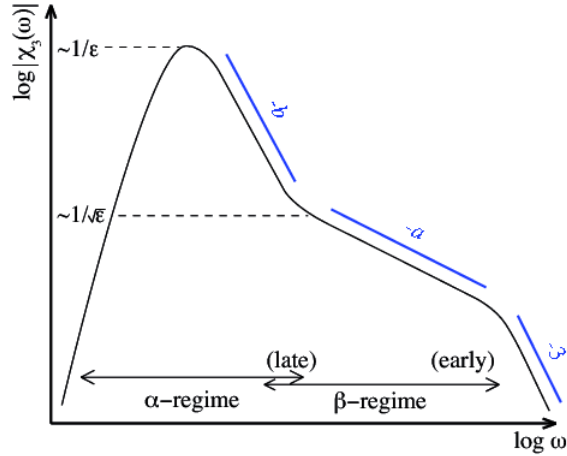


**Fig. 0.9** Sketch of  $\log |\chi_3(\omega)|$  as a function of  $\log \omega$ , showing different frequency regimes and crossovers (Tarzia *et al.*, 2010):  $\omega\tau_\alpha \ll 1$ ,  $\omega\tau_\alpha \sim 1$ ,  $\tau_\beta/\tau_\alpha \ll \omega\tau_\beta \ll 1$  ( $\epsilon = T - T_c$ ),  $\omega\tau_\beta \gg 1$ ,  $\omega\tau_0 \sim 1$ . Note that the low frequency limit is non zero but much smaller than the peak value for  $T$  close to  $T_c$ .

$$\chi_3(\omega) \approx \kappa \frac{\partial \chi_1(2\omega)}{\partial T}, \quad (0.23)$$

which is expected to hold at low enough frequency, at least when the deviations from time temperature superposition are weak.  $\kappa$  is expected to be a slowly varying function of temperature, a constant in first approximation (Tarzia *et al.*, 2010). In this expression,  $\partial \chi_1(\omega)/\partial T$  is akin to the three-point susceptibility  $\chi_T$  defined in section 0.2.5. Thus, Eq. (0.23) is an important result since it establishes a relationship with the linear dynamical responses that have been used to evaluate dynamical correlations, and it also proves that supercooled liquids should respond in an increasingly non-linear way approaching the glass transition since, as we have discussed before,  $\chi_T$  and therefore  $\frac{\partial \chi_1(2\omega)}{\partial T}$  increase approaching the glass transition.

The above general heuristic arguments can be supplemented by more microscopic ones based on MCT, which provides quantitative predictions on the critical behaviour of  $\chi_3$ . Although the corresponding results are restricted to the small temperature regime where MCT is believed to apply, they are nevertheless guidelines for the general behaviour of  $\chi_3$ . We sketch the evolution of the absolute value of  $\chi_3$  with frequency in Fig. 0.9.

- In the  $\alpha$ -regime, i.e.  $\omega \sim 1/\tau_\alpha \sim \epsilon^{1/2a+1/2b}/\tau_0$ , the absolute value of  $\chi_3(\omega)$  grows with decreasing  $\omega$  and reaches its maximum, of height of order  $1/\epsilon$ , after which it decreases as  $\omega^{-b}\tau_\beta$  at large  $\omega$ . In this regime, one has the scaling form:  $\chi_3(\omega) = \frac{1}{\epsilon} \mathcal{G}(\omega\tau_\alpha)$ .
- At the crossover between the early  $\alpha$ -regime and late  $\beta$ -regime the absolute value of  $\chi_3(\omega)$  is of order  $1/\sqrt{\epsilon}$ .

- In the  $\beta$ -regime, i.e.  $\omega \sim 1/\tau_\beta \sim \epsilon^{1/2a}/\tau_0$ , the absolute value of  $\chi_3(\omega)$  decreases as  $\omega^{-b}\tau_\beta$  at small  $\omega$  and as  $\omega^{-a}\tau_\beta$  at large  $\omega$ . In this regime one has a scaling form  $\chi_3(\omega) = \frac{1}{\sqrt{\epsilon}}\mathcal{F}(\omega\tau_\beta)$

Exponents  $a$  and  $b$  are the well known critical exponents of MCT introduced above;  $\tau_0$  is a microscopic relaxation time and  $\epsilon = (T - T_c)/T_c$  is the distance from the mode-coupling critical temperature  $T_c$ . We remark that the existence of the peak and the decrease at low frequency is a non trivial prediction since it is in contrast with the (trivial) non-linear response of uncorrelated Brownian dipoles (Déjardin and Kalmykov, 1999) and with spin glasses. The decrease with an exponent three at high frequency sketched in Fig. 0.9 is instead trivial and present also for independent dipoles (Déjardin and Kalmykov, 1999).

Recent experiments of third-order non-linear dielectric responses of supercooled glycerol have indeed shown, for the first time, that these theoretical expectations are qualitatively correct (Crauste-Thibierge *et al.*, 2010). We refer to the chapter by Alba-Simionesco *et al.* for a presentation of these experimental results and their discussion.

We conclude this section by emphasising that perturbing fields, other than electric fields, are expected to lead to similar results. Studying non-linear responses seems to us a very promising route to follow in order to probe the glassy state in a new way. A particularly interesting case worth studying corresponds to non-linear mechanical responses of colloidal glassy liquids. In this case, the values of the perturbing field that affect the sample are of the order of Pa, thus much smaller than the ones affecting the measuring apparatus, which are of the order of GPa. Thus, within a very good approximation, the only non-linear output signal is from the sample itself. This is not the case for dielectric measurements, which are therefore very difficult since one has to be able to filter out the trivial non-linear part due to the amplifiers, etc. This was the main difficulty in the experiment reported in (Crauste-Thibierge *et al.*, 2010).

#### 0.4.2 Inhomogeneous dynamical susceptibilities

We have seen in section 0.2.5 that the variation of a dynamical correlator with respect to an external parameter (e.g.,  $\chi_T$ ) is a way to obtain estimates of the number of dynamically correlated particles. As a natural generalisation, one can study the variation of a local correlator, which measures the dynamics around the position  $\mathbf{x}$ , induced by a perturbation at certain other point  $\mathbf{z}$ . By summing over all  $\mathbf{z}$  one obtains again a global dynamical response such as  $\chi_T$ , since this then corresponds to computing the variation with respect to a uniform shift of the external parameter.

This new, spatially dependent, dynamical response function is akin to  $G_4$  and allows one to probe the spatial structure of dynamic heterogeneity and to measure directly a dynamical correlation length  $\xi$ . The physical reason is that *spontaneous* dynamical fluctuations measured by the 4-point function and *induced* dynamical fluctuations measured by this new type of response function are intimately related. Accelerating or slowing down the dynamics at one given point (by adding an external potential) must perturb the dynamics over a length scale  $\xi$  if the dynamics are indeed correlated over this distance.

Let us define more precisely this new dynamical response. Consider the change in the local dynamical structure factor  $F(\mathbf{x}, \mathbf{y}, t)$  due to an extra, spatially varying, external potential  $U(\mathbf{z})$ . Note that this observable can always be decomposed in

Fourier modes:  $\frac{\delta F(\mathbf{x}, \mathbf{y}, t)}{\delta U(\mathbf{z})} \Big|_{U=0} = \int d\mathbf{k} d\mathbf{q} e^{-i\mathbf{q}\cdot(\mathbf{x}-\mathbf{y})+i\mathbf{k}\cdot(\mathbf{y}-\mathbf{z})} \chi_{\mathbf{k}}(\mathbf{q}, t)$ , where  $\chi_{\mathbf{k}}(\mathbf{q}, t) \propto \frac{\delta F(\mathbf{q}, \mathbf{q}+\mathbf{k}, t)}{\delta U(\mathbf{k})} \Big|_{U=0}$  is the response of the dynamical structure factor to a static external perturbation in Fourier space. For a perturbation localised at the origin,  $U(\mathbf{z}) = U_0 \delta(\mathbf{z})$ , one finds  $\delta F(\mathbf{q}, \mathbf{y}, t) = U_0 \int d\mathbf{k} e^{i\mathbf{k}\cdot\mathbf{y}} \chi_{\mathbf{k}}(\mathbf{q}, t)$ . This susceptibility is also related to a 3-point density correlation function in the absence of the perturbation. It is very important to note the very different role played by  $\mathbf{q}$  (the standard wavevector) and  $\mathbf{k}$  (the wavevector of the perturbation): only the latter is sensitive to dynamic correlations.<sup>5</sup>

The susceptibility  $\chi_{\mathbf{k}}(\mathbf{q}, t)$  is interesting for experimental reasons, at least in colloids, since it could be measured by using optical tweezer techniques. From a fundamental point view, it provides a very useful way to characterise dynamic heterogeneity since it is not affected by complications due to conservation laws and the type of dynamics, contrary to  $\chi_4$  and  $G_4$ . Therefore we expect that extracting spatial information and, especially, a precise estimate of  $\xi$  should be cleaner by using  $\chi_{\mathbf{k}}(\mathbf{q}, t)$  (see the discussion in section 0.2.6).

Finally, another advantage of  $\chi_{\mathbf{k}}(\mathbf{q}, t)$  is that precise quantitative predictions have been obtained within MCT by analytical arguments (Biroli *et al.*, 2006), which were later confirmed by numerical analysis (Szamel and Flenner, 2009) and complementary approaches (Szamel, 2008). The critical behaviour of  $\chi_{\mathbf{k}}(\mathbf{q}, t)$  approaching the MCT transition temperature is the following (we use the same MCT notation introduced previously):

- In the  $\beta$ -regime, i.e for times of the order of  $\tau_\beta = \epsilon^{-1/2a}$ , one finds

$$\chi_{\mathbf{k}}(\mathbf{q}, t) \propto \frac{1}{\sqrt{\epsilon} + \Gamma k^2} g_\beta \left( \frac{k^2}{\sqrt{\epsilon}}, t\epsilon^{1/2a} \right), \quad (0.24)$$

where the proportionality constant depends on  $q$ . The scaling function  $g_\beta(k^2/\sqrt{\epsilon}, t\epsilon^{1/2a})$  is regular for  $k = 0$ , thus implying that the  $\mathbf{k} = 0$  value diverge as  $1/\sqrt{\epsilon}$ . For large values of  $u = t\epsilon^{1/2a}$  one finds that  $g_\beta(k^2/\sqrt{\epsilon}, t\epsilon^{1/2a})$  equals  $\Xi(\Gamma k^2/\sqrt{\epsilon})u^b$ , with  $\Xi$  a certain regular function.

- In the  $\alpha$ -regime, i.e. for times of the order of  $\tau_\alpha = \epsilon^{-1/2a-1/2b}$ , one finds

$$\chi_{\mathbf{k}}(\mathbf{q}, t) = \frac{\Xi(\Gamma k^2/\sqrt{\epsilon})}{\sqrt{\epsilon}(\sqrt{\epsilon} + \Gamma k^2)} g_{\alpha, q} \left( \frac{t}{\tau_\alpha} \right) \quad (0.25)$$

with  $\Xi$  is the same function defined previously. It has the properties:  $\Xi(0) \neq 0$  and  $\Xi(v \gg 1) \sim 1/v$  such that  $\chi_{\mathbf{k}}$  behaves as  $k^{-4}$  for large  $k\epsilon^{-1/4}$ , independently of  $\epsilon$ . Also,  $g_{\alpha, q}(u \ll 1) \propto u^b$ , as to match the  $\beta$  regime, and  $g_{\alpha}(u \gg 1, k) \rightarrow 0$ .

Note that the spatial scaling variable is  $k^2/\epsilon^{-1/2}$  in both the  $\alpha$  and the  $\beta$  regimes. The physical consequence is that there exists a unique diverging dynamic correlation length  $\xi \sim \sqrt{\Gamma}|\epsilon|^{-1/4}$  that rules the response of the system to a space-dependent perturbation within MCT. The analysis of the early  $\beta$  regime where  $t \ll |\epsilon|^{-1/2a}$

<sup>5</sup>We note that compared to Refs. (Berthier *et al.*, 2007a, Biroli *et al.*, 2006), the notations  $\mathbf{q}$  and  $\mathbf{k}$  have been inverted.

shows that this length in fact first increases as  $t^{a/2}$  and then saturates at  $\xi$ . Interestingly, this suggests that while keeping a fixed extension  $\xi$ , the (fractal) geometrical structures carrying the dynamic correlations significantly “fatten” between  $\tau_\beta$  and  $\tau_\alpha$ , where more compact structures are expected, as perhaps suggested by the results of (Appignanesi *et al.*, 2006).

Up to now, there are no simulations or experiments measuring a spatial dynamic response such as  $\chi_{\mathbf{k}}(\mathbf{q}, t)$ . Hopefully, these will be performed in the future. As discussed previously, we do believe that this new observable is a simpler and more direct measure of dynamical correlations than  $G_4$ . Furthermore, quantitative results beyond scaling can be obtained within MCT. Thus one could consider comparing the MCT predictions for dynamical heterogeneities to numerical and experimental result in a stringent way, as it has been done for the intermediate scattering function, see e.g. (Kob and Andersen, 1995).

#### 0.4.3 Structure and dynamics: Is dynamic heterogeneity connected to the liquid structure?

One of the most frequently asked questions in studies of dynamical heterogeneity is whether the observed fluctuations might be structural in origin. Such questions have attracted sustained interest. For example, in early numerical work on dynamic heterogeneity, immobile regions were discussed in connection with compositional fluctuations in fluid mixtures (Hurley and Harrowell, 1995). Thirteen years later, some form of local crystalline order is invoked to account for slow domains in numerical work (Kawasaki *et al.*, 2007).

It should be noted that this chapter, and perhaps even this whole book about ‘dynamic heterogeneity’ would not exist in this form if the question of the connection between structure and dynamics had been satisfactorily answered. In that case, indeed, research would be dedicated to understanding the development of structural correlations at low temperatures in supercooled liquids, and to developing tools to measure, quantify and analyse such static features.

A key advance in connecting structural properties to dynamical heterogeneity has been the development of the so-called ‘isoconfigurational ensemble’ (Widmer-Cooper *et al.*, 2004). In this approach, one calculates a traditional ensemble average in two stages. First, one averages the particles’ velocities, keeping their initial positions fixed. (If the dynamics are stochastic, this step also contains an average over random noises.) Averaging a local dynamical observable such as  $c(r; t, 0)$  in this way, one arrives at an ‘isoconfigurational average’  $\langle c(r; t, 0) \rangle_{\text{iso}}$ , which still depends on the position  $r$  through the fixed initial particle positions. This average is therefore able to reveal the influence of the structure of the initial configuration on the dynamical behavior at that point. To return to a traditional ensemble average, one carries out an average over the initial particle positions in a second step.

The right panel of Fig. 0.1 represents the spatial dependence of the isoconfigurationally averaged single-particle mobility in a two-dimensional mixture of soft disks (Widmer-Cooper *et al.*, 2004). The fact that this image is not uniform demonstrates that part of the dynamic heterogeneity has a structural origin. This raises two different questions. First, can one predict from structural measurements the pattern

produced by the isoconfigurational average in Fig. 0.1? Second, how much of the ‘real’ dynamic heterogeneity is actually preserved by the isoconfigurational average and has thus a genuine structural origin?

Harrowell and coworkers have provided detailed answers to the first question (Widmer-Cooper *et al.*, 2004, Widmer-Cooper and Harrowell, 2006, Widmer-Cooper and Harrowell, 2005, Widmer-Cooper and Harrowell, 2007). Statistical analysis of isoconfigurational ensembles has been very useful in assessing the statistical significance of correlations between mobility and the local energy, composition or free volume. They have recently made the point that strong correlations exist between vibrational properties of the liquid and isoconfigurational mobilities (Widmer-Cooper *et al.*, 2008). They have also made vivid the distinction between the existence of a statistical correlation between structural and dynamical fluctuations, and the much more demanding notion of a causal link between the two, that is, of a correlation that is strong enough that prediction of the mobility can be made based on a given structural information (Widmer-Cooper and Harrowell, 2006, Widmer-Cooper and Harrowell, 2005). These two notions are very often confused in the dynamic heterogeneity literature.

The example of enthalpy fluctuations is useful in this respect. The fact that the four-point susceptibility  $\chi_4(t)$  can be quantitatively estimated with good accuracy from a three-point susceptibility such as  $\chi_T(t) \propto \langle \delta H(0) \delta C(t, 0) \rangle$  provides evidence of a strong correlation between enthalpy and dynamic fluctuations. However, enthalpy fluctuations are not good predictors for dynamic heterogeneity, presumably because they contain short-ranged and short-lived fluctuations that do not correlate well with slow dynamics. Indeed, suitably filtered enthalpy fluctuations correlate very strongly with dynamic heterogeneity (Matharoo *et al.*, 2006).

We finally return to the second question: is dynamic heterogeneity truly captured by isoconfigurational averages, and thus does it fully originate from the structure? The response is more subtle than expected as it depends on which observable, and more precisely on which lengthscale, it is analysed. We mentioned above that dynamic heterogeneity primarily revealed itself through the intermittent single particle dynamics (Fig. 0.3) leading to broad distributions of single particle displacements with broad tails. These features almost completely disappear after the isoconfigurational average is performed (Berthier and Jack, 2007). In other words, the distinction between mobile and immobile particles is mostly dynamical in nature, suggesting that the quest for a connection between the static and dynamic properties of glass-formers at the particle level is in vain.

Nevertheless, mobility fluctuations do display interesting spatial correlations, as illustrated in Fig. 0.1. This suggests that the distinction between fast and slow domains remains consistent in the isoconfigurational ensemble. This observation can be quantified by measuring a ‘restricted’ four-point function

$$\chi_4^{\text{iso}}(t) = N \left\langle \left( \langle C(t, 0)^2 \rangle_{\text{iso}} - \langle C(t, 0) \rangle_{\text{iso}}^2 \right) \right\rangle_{\text{initial cond.}}. \quad (0.26)$$

While  $\chi_4(t)$  measures the total strength of dynamic heterogeneity,  $\chi_4^{\text{iso}}(t)$  makes use of the isoconfigurational ensemble and first records the strength of dynamic heterogeneity at fixed initial conditions, the average over initial conditions being performed after-

wards. In the case where isoconfigurational mobility (and thus the image in Fig. 0.1) is uniform, one has  $\chi_4^{\text{iso}}(t) = \chi_4(t)$ , since the average over initial conditions is trivial in this case. More generally, a large contribution of  $\chi_4^{\text{iso}}(t)$  to  $\chi_4(t)$  indicates that the dynamic fluctuations captured by  $\chi_4(t)$  are inherently dynamical in origin and do not originate in the liquid structure. Numerical measurements in molecular dynamics simulations indicate that the opposite is true and  $\chi_4^{\text{iso}}(t)$  contributes less and less to  $\chi_4(t)$  as temperature decreases (Berthier and Jack, 2007). This suggests that the search of a causal link between structure and mobility does make sense, at least on large length scales. Interestingly, the vibrational properties investigated in Ref. (Widmer-Cooper *et al.*, 2008) as relevant structural indicators of dynamic heterogeneity are a suitable candidate, since the vibrational spectrum is a collective property.

#### 0.4.4 Point to set correlations: Emergence of amorphous long range order?

As discussed in the previous section, it is quite natural to ask what structural features (if any) might be responsible for the growth of dynamical correlations. One possibility is that actually there exists a static growing length that drives the increase of dynamical correlations. As we discussed in the introduction, simple static correlations are rather featureless when approaching the glass transition. However a new length called the “point to set” length was recently introduced (Bouchaud and Biroli, 2004, Mézard and Montanari, 2006). It is naturally devised to probe the growth of static amorphous long range order (Bouchaud and Biroli, 2004, Mézard and Montanari, 2006) and has been shown to grow close to the glass transition (Biroli *et al.*, 2008). This is reviewed in the chapter by Semerjian and Franz.

The basic idea is to measure how much boundary conditions affect the behaviour of the system, far away from the boundaries themselves. This is the usual way to test for the emergence of long range order in statistical mechanics. However, for standard phase transitions, the appropriate boundary conditions are known from the outset. For example, in the case of ferromagnetic transitions, one can fix the boundary spins mostly in the up direction and check whether this leads to a positive magnetisation for spins in the bulk. The difficulty in the case of glasses, for which one would like to test the presence of long range amorphous order, is that the boundary conditions one has to use look just as random as the amorphous configuration one wants to select. The way out is to let the system itself choose the boundary conditions: the procedure is to take an equilibrated configuration  $\alpha$ , freeze all particles outside a cavity of radius  $\mathcal{R}$  and then recompute the thermodynamics for the particles inside the cavity, that now are subjected to a typical equilibrium boundary condition. One can then study a suitably defined average overlap  $q(\mathcal{R})$  between the new thermalized configurations at the centre of the cavity and the reference state  $\alpha$ , as a function of  $\mathcal{R}$ . The quantity  $q(\mathcal{R})$  is called a “point-to-set” correlation (Mézarad and Montanari, 2006). The characteristic length scale over which  $q(\mathcal{R})$  drops to zero is called the point to set length. The increase of this length is a clear signal that the system is developing long range static order, and in the case of glasses, amorphous long range order. This point-to-set length is precisely the size of the glassites within the RFOT theory of glasses, see section 0.3.2.

This topic is discussed in detail by Franz and Semerjian, to which we refer for a presentation of the general theoretical and numerical results. Here we simply mention that this point to set length has been shown to grow in numerical simulations of supercooled liquids (Biroli *et al.*, 2008). Furthermore, it was proved that it must diverge whenever the relaxation time does so (Montanari and Semerjian, 2006).

Therefore, an important open question is whether the correlation length picked up by the dynamical correlators discussed above are actually just a consequence of hidden static correlations or if they are instead quite unrelated to them. In the first case, the study of dynamical correlation will still be very valuable because it provides an easier way to probe static correlations. Whatever is the correct answer, it would lead to a substantial progress in our understanding of the glass transition and would help us in pruning down the correct theory. We do hope that numerical and experimental studies will be devoted to this important problem in the future.

#### 0.4.5 Large deviations and space-time thermodynamics

It is clear from its definition in Eq. (0.7) that the correlation  $G_4(r, t)$  is the covariance of the mobility  $c(r; 0, t)$  at two nearby spatial points. Similarly, the three-point functions of the previous section are covariances of  $c(r; 0, t)$  with the local energy, enthalpy or free volume. Of course, not all information about the mobility is contained in such covariances: one might consider higher moments of these functions or indeed the joint distribution of mobilities at all points. However, the inherent difficulty of characterising the distribution of an entire mobility field requires physical intuition in choosing which observable to measure.

A natural first choice for such a scheme is to consider the fluctuations of the spatially averaged correlation function  $C(t, 0)$ , beyond the Gaussian level. Such measurements are possible in experiments such as those of Duri *et al.* (Duri *et al.*, 2005) (see Fig. 0.10) and in computer simulations of a variety of models (Chamon *et al.*, 2004). They have typically been considered in out-of-equilibrium situations but this is not essential (see also below). Typically, such distributions are skewed and non-Gaussian, and it is natural to connect the asymmetry of the distribution with dynamical heterogeneity. For example, even on time scales  $t$  much greater than the structural relaxation time, there is a substantial probability that regions of the system have persisted in an immobile state for all times between 0 and  $t$ . This enhances the probability of observing a larger than average value for  $C(t, 0)$ . The opposite behaviour may occur on short times: while typical regions have not relaxed, co-operative motion in some regions enhances the probability of observing a smaller than average of  $C(t, 0)$ .

In making this connection, it seems reasonable that regions where  $C(t, 0)$  is large possess rather stable structure at the molecular level, while regions where  $C(t, 0)$  is small correspond to relatively unstable local structure. This fact has recently been exploited in computational studies that probe trajectories where relaxation is much slower than average. To identify such trajectories, it is useful to define a measure of dynamical activity, for systems of  $N$  particles evolving over an observation time  $t_{\text{obs}}$ . For example, one may take (Hedges *et al.*, 2009)

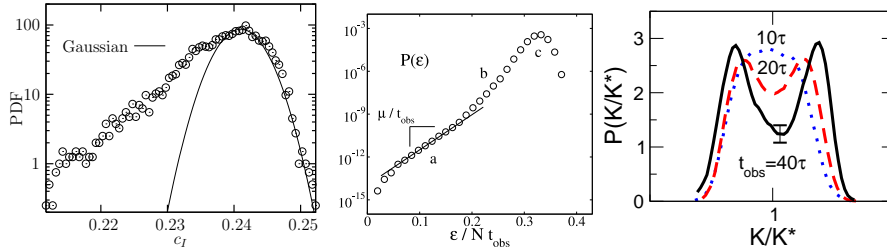


**Fig. 0.10** Distributions of dynamical observables. (Left) Distribution of the correlation function in a coarsening foam (Duri *et al.*, 2005). The skewed distribution arises from rare trajectories with more motion than average. (Centre) The distribution of the ‘dynamical action’  $\epsilon$  in a kinetically constrained model (Merolle *et al.*, 2005). The action  $\epsilon$  measures the amount of motion in a trajectory in the same spirit as the activity  $K$  defined in Eq. (0.27). The distribution is left-skewed and non-convex, indicating a population of trajectories with low mobility. (Right) Distribution of the activity  $K$  in a model of Lennard-Jones particles, with a biasing field  $s$  in place, as discussed in the text. Two peaks are evident when the  $t_{\text{obs}}$  is large, revealing the presence of two distinct dynamical phases (Hedges *et al.*, 2009).

$$K(N, t_{\text{obs}}) = \sum_{i=1}^N \sum_{j=1}^{t_{\text{obs}}/\Delta t} |\mathbf{r}_i(t_j) - \mathbf{r}_i(t_j - \Delta t)|^2, \quad (0.27)$$

where  $\mathbf{r}_i(t)$  is the position of particle  $i$  at time  $t$  and the  $t_j = j\Delta t$  are equally spaced times. For large  $N$  and  $t_{\text{obs}}$ , the distribution of  $K$  becomes sharply peaked about its average,  $\langle K \rangle$ .

In general, for large  $N$  and  $t_{\text{obs}}$ , one expects a the equilibrium distribution of  $K$  to have the form

$$P(K) \simeq \exp[-Nt_{\text{obs}}f(K/Nt_{\text{obs}})] \quad (0.28)$$

where the function  $f(k)$  resembles a free energy density: it gives the probability of observing a substantial deviation between the measured  $K$  and its average  $\langle K \rangle$ . (The variance of  $K$  was also considered in Ref. (Merolle *et al.*, 2005). In general, this quantity contains different information to four-point functions such as  $\chi_4(k, t)$  although  $\chi(t_{\text{obs}})$  and  $\chi_4(k, t)$  may sometimes be related through scaling arguments<sup>6</sup>.) In some kinetically constrained models (Merolle *et al.*, 2005), the distribution  $P(K)$  has a characteristic shape, skewed towards small activity, with an apparently exponential tail, as shown in the central panel of Fig. 0.10. Further, on estimating  $f(k)$  from this plot, there is a range of  $K$  over which  $f(k)$  is non-convex (that is,  $f''(K) < 0$ ). The behaviour of  $f(k)$  away from its minimum describes the properties of rare trajectories in the system and their relevance for the liquid behaviour is not clear *a priori*. However,

<sup>6</sup> In the notation of Eq. (0.7), one may write  $K = \sum_i \sum_j c_i(t_j, t_j + \Delta t)$  so that the variance of  $K$  contains terms like  $g_{ijmn} = \langle c_i(t_j, t_j + \Delta t)c_m(t_n, t_n + \Delta t) \rangle$ . Assuming that  $g_{ijmn}$  depends on scaling variables such as  $|r_i - r_j|/\xi_4$  and  $(t_j - t_n)/\tau_\alpha$ , one may connect the variance of  $K$  to the dynamical length scale  $\xi_4$  and time scale  $\tau_\alpha$ . Such connections are analogous to the relation (0.14) between  $\chi_4(t)$  and  $\xi_4(t)$ , but there is considerable freedom in the scaling ansatz for  $g_{ijmn}$ , which seems to prevent a more direct connection between the variance of  $K$  and  $\chi_4(t)$ .

the key motivation of this study was to formulate a thermodynamic approach to the statistical properties of trajectories of glassy systems (Garrahan and Chandler, 2002). Within such a framework, non-convexity of  $f(K)$  has a direct interpretation as a ‘dynamical phase transition’ in the system.

This interpretation is most easily seen by taking the Legendre transform of  $f(K)$  to obtain a new ‘dynamical free energy’

$$\psi(s) = -\min_k [sk + f(k)], \quad (0.29)$$

which describes the response of the system to a field  $s$  that biases the system towards trajectories with small (or large) activity  $K$ . In particular, the effect of the bias is to change the average of  $K$  from  $\langle K \rangle$  to  $K(s) = -Nt_{\text{obs}} \frac{d}{ds} \psi(s)$ . Then, a non-convex form for  $f(K)$  results in a jump singularity of  $K(s)$  for a specific biasing field  $s = s^*$ . While the field  $s$  has no simple physical interpretation, one may view it as a mathematically convenient trick for sampling the distribution  $P(K)$ .

Turning to the results of this formalism, the key point is that glassy systems may exhibit singular responses to the field  $s$ , leading to ‘ideal glass’ states that are characterised by values of  $K$  that is much smaller than its equilibrium average  $\langle K \rangle$ . The existence of these phase transitions has been proven in simple models (Garrahan *et al.*, 2007, Jack and Garrahan, 2010) and numerical results for Lennard-Jones model liquids are also consistent with the existence of such a transition (Hedges *et al.*, 2009). In particular, if the field  $s$  is chosen to lie at the putative phase transition point, then one may construct the distribution of  $K$  in the presence of the field  $s$ ,  $P_s(K) \propto P(K)e^{-sK}$ . In the presence of a phase transition,  $P_s(K)$  has two peaks, which correspond to distinct active (liquid) and inactive (glass) states. An example is shown in the right panel of Fig. 0.10.

To summarise then, dynamical heterogeneity is concerned with distributions of dynamical quantities, most often through their means and covariances. However, the tails of these distributions can reveal information about possible new phases in the system, whose structure is very stable and whose relaxation times are very long. This leads to the hypothesis that the nature of the dynamically heterogeneous fluid state should be interpreted in terms of coexistence between active liquid and inactive ‘ideal glass’ states.

## 0.5 Open problems and conclusions

The aim of this chapter was to review the recent progress in the quantitative analysis of dynamical heterogeneities. We showed that the introduction of four-point correlation functions played an important role, both conceptually and operationally, by providing a precise quantitative measure to characterise dynamical heterogeneities. These four-point correlations have now been measured or estimated in numerical simulations of schematic and realistic models of glass formers, and experimentally on molecular glasses, colloids and granular assemblies close to jamming. They have also been investigated theoretically within simplified models or within the mode-coupling approximation, and have indeed been shown to be critical as the glass transition is approached. These four-point correlations are the natural counterpart, for glass or

spin-glass transitions, of the standard two-point correlations that diverge close to a usual second-order phase transition. These can be considered to be breakthroughs that have significantly improved our understanding of the microscopic mechanisms leading to glass formation, and that have already spilled over to many different scientific communities.

However, it soon became clear that four-point correlation functions are not a panacea. It was for example not anticipated that these functions would be delicately sensitive to details such as the choice of statistical ensemble or the microscopic dynamics. Second, although these four-point objects give valuable information, they are not powerful enough to answer more precise questions about the geometry of the structures that carry dynamical heterogeneities, or about the nature of the relaxation events (continuous vs. activated). Along the same line of thought, the relation between the dynamical correlation length extracted from these four-point points and the intuitive (but not so clearly defined) notion of cooperative relaxation is at this stage quite elusive. How many different ‘dynamical’ length scales does one expect in general?

We have seen that the study of three-point response functions and non-linear susceptibilities allows one to bypass some of the difficulties inherent to four-point functions. We note that the experimental and numerical situation on that front is much less developed, and should be encouraged. The very recent measurement of the non-linear dielectric properties of glycerol (Crauste-Thibierge *et al.*, 2010) is a remarkable exception.

Higher-order correlation functions might also contain interesting quantitative information about dynamical heterogeneities, but this subject is at this stage totally unexplored. It was recently suggested (Lechenault *et al.*, 2010) that six-point functions might provide a way to measure intermittent dynamics and identify activated events. Skewness (or kurtosis) might indeed detect that the dynamics is intermittent, as one expects if ‘activated’ events dominate, with a few rare events decorrelating the system completely, while most events decorrelate only weakly. More work in that direction would certainly be worthwhile.

Finally, we have not touched upon the problem of out-of-equilibrium dynamical heterogeneities, in particular in the aging regime. This is clearly a very interesting topic, for which experimental efforts are underallocated, although results in this regime might be able to discriminate between theories. We refer to (Parisi, 1999, Castillo *et al.*, 2003, Parsaeian and Castillo, 2008, Vollmayer-Lee *et al.*, 2002, Vollmayer-Lee and Baker, 2006, El Masri *et al.*, 2010, Courtland and Weeks, 2003) and the chapter on aging in this book for interesting lines of research on this issue in spin-glasses.

# References

- Adam, G. and Gibbs, J. H. (1965). *J. Chem. Phys.*, **43**, 139.
- Appignanesi, G. A., Rodríguez Fris, J. A., Montani, R. A., and Kob, W. (2006). *Phys. Rev. Lett.*, **96**, 057801.
- Bennemann, C., Donati, C., Baschnagel, J., and Glotzer, S. C. (1999). *Nature*, **399**, 246.
- Berthier, L. (2003). *Phys. Rev. Lett.*, **91**, 055701.
- Berthier, L. (2004). *Phys. Rev. E*, **69**, 020201(R).
- Berthier, L. (2007). *Phys. Rev. E*, **76**, 011507.
- Berthier, L., Biroli, G., Bouchaud, J.-P., Cipelletti, L., El Masri, D., L'Hôte, D., Ladieu, F., and Pierno, M. (2005). *Science*, **310**, 1797.
- Berthier, L., Biroli, G., Bouchaud, J.-P., Kob, W., Miyazaki, K., and Reichman, D. R. (2007a). *J. Chem. Phys.*, **126**, 184503.
- Berthier, L., Biroli, G., Bouchaud, J.-P., Kob, W., Miyazaki, K., and Reichman, D. R. (2007b). *J. Chem. Phys.*, **126**, 184504.
- Berthier, L. and Garrahan, J. P. (2005). *J. Phys. Chem. B*, **109**, 3578.
- Berthier, L. and Jack, R. L. (2007). *Phys. Rev. E*, **76**, 041509.
- Berthier, L. and Kob, W. (2007). *J. Phys.: Condens. Matter*, **19**, 205130.
- Binder, K. and Kob, W. (2005). *Glassy materials, and disordered solids*. World Scientific, Singapore.
- Biroli, G. and Bouchaud, J.-P. (2004). *Europhys. Lett.*, **67**, 21.
- Biroli, G. and Bouchaud, J.-P. (2009). *arXiv:0912.2542*.
- Biroli, G., Bouchaud, J.-P., Cavagna, A., Grigera, T. S., and Verrocchio, P. (2008). *Nature Phys.*, **4**, 771.
- Biroli, G., Bouchaud, J.-P., and Miyazaki, K. (2006). *and D. R. Reichman Phys. Rev. Lett.*, **97**, 195701.
- Bouchaud, J.-P. and Biroli, G. (2004). *J. Chem. Phys.*, **121**, 7347.
- Bouchaud, J.-P. and Biroli, G. (2005). *Phys. Rev. B*, **72**, 064204.
- Brambilla, G., El Masri, D., Pierno, M., Petekidis, G., Schofield, A. B., Berthier, L., and Cipelletti, L. (2009). *Phys. Rev. Lett.*, **102**, 085703.
- Capaccioli, S., Ruocco, G., and Zamponi, F. (2008). *J. Phys. Chem. B*, **112**, 10652.
- Castillo, H., Chamon, C., Cugliandolo, L. F., Iguain, J. L., and Kennett, M. P. (2003). *Phys. Rev. B*, **68**, 134442.
- Chamon, C., Charbonneau, P., Cugliandolo, L. F., and Reichman, D. R. (2004). *J. Chem. Phys.*, **121**, 10120.
- Chandler, D. and Garrahan, J. P. (2010). *Annu. Rev. Phys. Chem.*, **61**, 191.
- Chandler, D., Garrahan, J. P., Jack, R. L., Maibaum, L., and Pan, A. C. (2006). *Phys. Rev. E*, **74**, 051501.
- Chaudhuri, P., Berthier, L., and Kob, W. (2007). *Phys. Rev. Lett.*, **99**, 060604.

- Courtland, R. E. and Weeks, E. R. (2003). *J. Phys.: Condens. Matter*, **15**, S359.
- Crauste-Thibierge, C., Brun, C., Ladieu, F., L'Hôte, D., Biroli, G., and Bouchaud, J.-P. (2010). *Phys. Rev. Lett.*, **104**, 165703.
- Dalle-Ferrier, C., Thibierge, C., Alba-Simionesco, C., Berthier, L., Biroli, G., Bouchaud, J.-P., Ladieu, F., L'Hôte, D., and Tarjus, G. (2007). *Phys. Rev. E*, **76**, 041510.
- Dasgupta, C., Indrani, A. V., Ramaswamy, S., and Phani, N. K. (1991). *Europhys. Lett.*, **15**, 307.
- Dauchot, O., Marty, G., and Biroli, G. (2005). *Phys. Rev. Lett.*, **95**, 265701.
- Debenedetti, P. G. (1996). *Metastable liquids*. Princeton University Press, Princeton.
- Déjardin, J. L. and Kalmykov, Yu. P. (1999). *Phys. Rev. E*, **61**, 1211.
- Doliwa, B. and Heuer, A. (2000). *Phys. Rev. E*, **61**, 6898.
- Donati, C., Douglas, J. F., Kob, W., Plimpton, S. J., Poole, P. H., and Glotzer, S. C. (1998). *Phys. Rev. Lett.*, **80**, 2338.
- Donati, C., Glotzer, S.C., and Poole, P.H. (1999). *Phys. Rev. Lett.*, **82**, 5064.
- Duri, A., Bissig, H., Trappe, V., and Cipelletti, L. (2005). *Phys. Rev. E*, **72**, 051401.
- Duri, A. and Cipelletti, L. (2006). *Europhys. Lett.*, **76**, 972.
- Ediger, M. D. (2000). *Annu. Rev. Phys. Chem.*, **51**, 99.
- Edwards, S. F. and Anderson, P. W. (1975). *J. Phys. F: Metal Phys.*, **5**, 965.
- El Masri, D., Berthier, L., and Cipelletti, L. (2010). *Phys. Rev. E (in press)*; [arxiv.org:1006.4422](http://arxiv.org/1006.4422).
- Fernandez, L. A., Martin-Mayor, V., and Verrocchio, P. (2006). *Phys. Rev. E*, **73**, 020501.
- Fischer, K. H. and Hertz, J. A. (1991). *Spin Glasses*. Cambridge University Press, Cambridge.
- Flenner, E. and Szamel, G. (2009). *Phys. Rev. E*, **79**, 051502.
- Flenner, E. and Szamel, G. (2010). [arxiv:1005.3794](http://arxiv.org/1005.3794).
- Franz, S., Donati, C., Parisi, G., and Glotzer, S. C. (1999). *Philos. Mag. B*, **79**, 1827.
- Franz, S. and Parisi, G. (2000). *J. Phys.: Condens. Matter*, **12**, 6335.
- Garrahan, J. P. and Chandler, D. (2002). *Phys. Rev. Lett.*, **89**, 035704.
- Garrahan, J. P. and Chandler, D. (2003). *Proc. Nat. Acad. Sci. USA*, **100**, 9710.
- Garrahan, J. P., Jack, R. L., Lecomte, V., Pitard, E., van Duijvendijk, K., and van Wijland, F. (2007). *Phys. Rev. Lett.*, **98**, 195702.
- Glarum, S. H. (1960). *J. Chem. Phys.*, **33**, 1371.
- Glotzer, S. C., Novikov, V., and Schroder, T. B. (2000). *J. Chem. Phys.*, **112**, 509.
- Götze, W. (2008). *Complex dynamics of glass-forming liquids: A mode-coupling theory*. Oxford University Press, Oxford.
- Götze, W. and Sjögren, L. (1995). *Rep. Prog. Phys.*, **55**, 241.
- Hansen, J. P. and McDonald, I. R. (1986). *Theory of Simple Liquids*. Academic, London.
- Hedges, L. O., Jack, R. L., Garrahan, J. P., and Chandler, D. (2009). *Science*, **323**, 16665.
- Hedges, L. O., Maibaum, L., Chandler, D., and Garrahan, J. P. (2007). *J. Chem. Phys.*, **127**, 211101.
- Heuer, A. (2008). *J. Phys.: Condens. Matter*, **20**, 373101.

- Heussinger, C., Berthier, L., and Barrat, J.-L. (2010). *EPL*, **90**, 20005.
- Hurley, M. M. and Harrowell, P. (1995). *Phys. Rev. E*, **52**, 1694.
- Jack, R. L. and Garrahan, J. P. (2010). *Phys. Rev. E*, **81**, 011111.
- Jack, R. L., Mayer, P., and Sollich, P. (2006). *J. Stat. Mech.*, P03006.
- Jung, Y., Garrahan, J.P., and Chandler, D. (2004). *Phys. Rev. E*, **69**, 061205.
- Karmakar, S., Dasgupta, C., and Sastry, S. (2009). *Proc. Natl. Acad. Sci. USA*, **106**, 3675.
- Kawasaki, T., Araki, T., and Tanaka, H. (2007). *Phys. Rev. Lett.*, **99**, 215701.
- Kegel, W. K. and van Blaaderen, A. (2000). *Science*, **287**, 290.
- Keys, A. S., Abate, A. R., Glotzer, S. C., and Durian, D. J. (2007). *Nature Phys.*, **3**, 260.
- Kirkpatrick, T. R., Thirumalai, D., and Wolynes, P. G. (1989). *Phys. Rev. A*, **40**, 1045.
- Kob, W. and Andersen, H. C. (1995). *Phys. Rev. E*, **51**, 4626.
- Kob, W., Donati, C., Plimpton, S. J., Poole, P. H., and Glotzer, S. C. (1997). *Phys. Rev. Lett.*, **79**, 2827.
- Lacevic, N., Starr, F. W., Schroder, T. B., and Glotzer, S. C. (2003). *J. Chem. Phys.*, **119**, 7372.
- Lacevic, N., Starr, F. W., Schroder, T. B., Novikov, V. N., and Glotzer, S. C. (2002). *Phys. Rev. E*, **66**, 030101.
- Lechenault, F., Candelier, R., Dauchot, O., Bouchaud, J.-P., and Biroli, G. (2010). *Soft Matter*, **6**, 3059.
- Lechenault, F., Dauchot, O., Biroli, G., and Bouchaud, J.-P. (2008a). *EPL*, **83**, 46003.
- Lechenault, F., Dauchot, O., Biroli, G., and Bouchaud, J.-P. (2008b). *EPL*, **83**, 46002.
- Lubchenko, V. and Wolynes, P.G. (2006). *Ann. Rev. Phys. Chem.*, **58**, 235.
- Lunkenheimer, P. and Loidl, A. (2002). *Chem. Phys.*, **284**, 205.
- Mapes, M. K., Swallen, S. F., and Ediger, M. D. (2006). *J. Chem. Phys.*, **124**, 054710.
- Marty, G. and Dauchot, O. (2005). *Phys. Rev. Lett.*, **94**, 015701.
- Matharoo, G. S., Razul, M. S. G., and Poole, P. H. (2006). *Phys. Rev. E*, **74**, 050502.
- Mayer, P., Bissig, H., Berthier, L., Cipolletti, L., Garrahan, J. P., Sollich, P., and Trappe, V. (2004). *Phys. Rev. Lett.*, **93**, 115701.
- Menon, N. and Nagel, S. R. (1995). *Phys. Rev. Lett.*, **74**, 1230.
- Merolle, M., Garrahan, J. P., and Chandler, D. (2005). *Proc. Natl. Acad. Sci. USA*, **102**, 10837.
- Mézard, M. and Montanari, A. (2006). *J. Stat. Phys.*, **124**, 1317.
- Mézard, M., Parisi, G., and Virasoro, M. (1988). *Spin glass Theory, and Beyond*. World Scientific, Singapore.
- Montanari, A. and Semerjian, G. (2006). *J. Stat. Phys.*, **125**, 23.
- Pan, A. C., Garrahan, J. P., and Chandler, D. (2005). *Phys. Rev. E*, **72**, 041106.
- Parisi, G. (1999). *J. Chem. Phys. B*, **103**, 4128.
- Parsaeian, A. and Castillo, H. E. (2008). *Phys. Rev. E*, **78**, 060105(R).
- Reinsberg, S. A., Qiu, X. H., Wilhelm, M., Spiess, H. W., and Ediger, M. D. (2001). *J. Chem. Phys.*, **114**, 7299.
- Richert, R. (2002). *J. Phys.: Condens. Matter*, **14**, R703.
- Richert, R., Israeloff, N., Alba-Simionesco, C., Ladieu, F., and L'Hôte, D. (2010).

## Chapter 4.

- Ritort, F. and Sollich, P. (2003). *Adv. Phys.*, **52**, 219.
- Sillescu, H. (1999). *J. Non-Cryst. Solids*, **243**, 81.
- Stein, R. S. L. and Andersen, H. C. (2008). *Phys. Rev. Lett.*, **101**, 267802.
- Stevenson, J. D., Schmalian, J., and Wolynes, P. G. (2006). *Nature Phys.*, **2**, 268.
- Stillinger, F. H. and Hodgdon, J. A. (1994). *Phys. Rev. E*, **50**, 2064.
- Szamel, G. (2008). *Phys. Rev. Lett.*, **101**, 205701.
- Szamel, G. and Flenner, E. (2009). *Phys. Rev. E*, **79**, 021503.
- Tarjus, G. (2010). *Chapter 1*.
- Tarjus, G. and Kivelson, D. (1995). *J. Chem. Phys.*, **103**, 3071.
- Tarzia, M., Biroli, G., Bouchaud, J.-P., and Lefèvre, A. (2010). *J. Chem. Phys.*, **132**, 054501.
- Toninelli, C., Wyart, M., Berthier, L., Biroli, G., and Bouchaud, J.-P. (2005). *Phys. Rev. E*, **71**, 041505.
- Tracht, U., Wilhelm, M., Heuer, A., Feng, H., Schmidt-Rohr, K., and Spiess, H. W. (1998). *Phys. Rev. Lett.*, **81**, 2727.
- Vidal Russell, E. and Israeloff, N. E. (2000). *Nature*, **408**, 695.
- Vogel, M. and Glotzer, S. C. (2004). *Phys. Rev. E*, **70**, 061504.
- Vollmayer-Lee, K. and Baker, E. A. (2006). *Europhys. Lett.*, **76**, 1130.
- Vollmayer-Lee, K., Kob, W., Binder, K., and Zippelius, A. (2002). *J. Chem. Phys.*, **116**, 5158.
- Weeks, E. R., Crocker, J. C., Levitt, A. C., Schofield, A., and Weitz, D. A. (2000). *Science*, **287**, 627.
- Weeks, E. R., Crocker, J. C., and Weitz, D. A. (2007). *J. Phys.: Condens. Matter*, **19**, 205131.
- Whitelam, S., Berthier, L., and Garrahan, J.P. (2004). *Phys. Rev. Lett.*, **92**, 185705.
- Whitelam, S., Berthier, L., and Garrahan, J.P. (2005). *Phys. Rev. E*, **71**, 026128.
- Widmer-Cooper, A. and Harrowell, P. (2005). *J. Phys.: Condens. Matter*, **17**, S4025.
- Widmer-Cooper, A. and Harrowell, P. (2006). *Phys. Rev. Lett.*, **96**, 185701.
- Widmer-Cooper, A. and Harrowell, P. (2007). *J. Chem. Phys.*, **126**, 154503.
- Widmer-Cooper, A., Harrowell, P., and Fynewever, H. (2004). *Phys. Rev. Lett.*, **93**, 135701.
- Widmer-Cooper, A., Perry, H., Harrowell, P., and Reichman, D. R. (2008). *Nature Phys.*, **4**, 711.
- Wuttke, J., Petry, W., and Pouget, S. (1996). *J. Chem. Phys.*, **105**, 5177.
- Xia, X. Y. and Wolynes, P. G. (2000). *Proc. Natl. Acad. Sci. USA*, **97**, 2990.
- Yamamoto, R. and Onuki, A. (1998a). *Phys. Rev. Lett.*, **81**, 4915.
- Yamamoto, R. and Onuki, A. (1998b). *Phys. Rev. E*, **58**, 3515.